PROFILES AND WAVELENGTHS OF SPECTRUM LINES IN THE SOLAR CHROMOSPHERE

Thesis by

James Mervin Parker

In Partial Fulfillment of the Requirements

for the Degree of

Doctor of Philosophy

California Institute of Technology

Pasadena, California

1954

Acknowledgments

It is a pleasure to express my sincere gratitude to Dr. Seth B. Nicholson for his consistent aid in obtaining the observations of the solar chromosphere, and for many helpful discussions during the earlier part of the work. I also wish to extend my thanks to Dr. Jesse L. Greenstein for his suggestions and guidance in the interpretation of the observations.

Abstract

Observations have been made of the spectrum of the solar chromosphere outside of eclipse. The spectral region covered extends from λ5000Å to λ5270Å, and from λ5440Å to λ6570Å. In addition, the O I triplet at λ7774Å was photographed. In all, 1882 emission lines were photographed, and measured for wavelengths. Photographic intensity profiles were found for 530 of the lines, through the use of a microdensitometer. 330 of these lines were due to the Swan bands of C_2. These lines were measured for total intensity, and a rotational temperature of 4600°K derived. The other 200 lines were reduced using the method of Voigt profiles. The width of the lines as a function of atomic weight was examined in the light of several assumptions, and it was found that the best interpretation was that of low temperature, of the order of 5000°K to 6000°K and an overlying turbulent motion which varies with height in the chromosphere. The interpretation of the line contours on this basis was performed using the model chromosphere due to van de Hulst.

TABLE OF CONTENTS

I. Introduction

The solar chromosphere may be roughly defined as that portion of the sun's atmosphere which lies in an intermediate position between the visual photosphere and the tenuous corona. There must, of course, be a continuous merging of the chromosphere into the photosphere and corona, and hence the upper and lower portions of the chromosphere must have characteristics closely resembling the corona and photosphere, respectively. Historically, the chromosphere was first observed at eclipses of the sun, where it appeared as a dark red crescent around the moon a few seconds before totality. In later years, when spectroscopic observations were made, this thin, short-lived crescent gave rise to the spectacular "flash spectrum", so called because of its extremely short duration. As the eclipse progresses toward totality, the chromospheric layers are covered by the encroaching moon, and the flash spectrum disappears, to reappear momentarily at the corresponding time just after totality. In the latter part of the 19th century, it was found that spectroscopic observations of the chromosphere were possible outside of an eclipse, by the simple expedient of placing the slit of the spectrograph very close to the limb of the sun. However, only the prominences and a few very strong lines which extend to great heights were seen. In 1909, however, Hale and Adams observed the spectrum from the lower chromosphere under fine seeing conditions; the spectrum appeared to be at least as rich in lines as under eclipse conditions. In 1915, Adams and Burwell published a list of some 1200 lines observed in the flash spectrum without eclipse, between the wavelengths of λ4800Å and λ6600Å. A large proportion of the stronger

lines seemed to exhibit the phenomenon of double reversal, in that they appeared in the chromosphere as absorption lines with their wings in emission. In this paper, Adams points out that the spectra are from the lower levels of the chromosphere, using among other bits of evidence the fact that the "Carbon flutings" are quite strong, and that from visual observations they are known to occur at low levels. Indeed, the eclipse observations show far fewer carbon lines than the observations made without eclipse, and hence at least from the visual observations mentioned above it would seem that the eclipse observations refer to a higher level in the chromosphere.

After 1915, no concerted effort was made to obtain the flash spectrum outside of eclipse until the work of H. W. Babcock, between 1932 and 1935, much of which remains unpublished. Babcock obtained excellent spectra from λ5000Å clear up to about λ10,000Å, at a dispersion of about 0.7Å/mm. Unfortunately, these plates were not calibrated, for the most part, and hence are not useful for photometric purposes.

A few individual observations of particular spectrum lines, notably of hydrogen and helium, have been carried out from time to time, but no complete series of observations over an extended wavelength region has been carried out since 1935. In view of the tremendous difficulties attending eclipse observations, it seems advisable to attempt to obtain calibrated plates of the flash spectrum outside of eclipse. A few of the obvious advantages of this type of observations include the higher resolution of the spectrographs available, and the fact that there is no time limit for an exposure, as there is in the case of eclipse observations. The obvious disadvantages include the notoriously poor daytime solar seeing, and the fact that the light from the limb of the

sun is not blocked out, and hence presents a very intense source of radiation in close proximity to the faintly radiating region of interest.

The present investigation was undertaken with the idea of determining the wavelengths and profiles of the lines in the flash spectrum without an eclipse, and hence to determine kinetic temperatures and turbulence, if any, in the lower chromosphere. Observations of a similar nature have been carried out at an eclipse, by Redman (1); the present observations are of higher dispersion, and in a different wavelength region, as well as being of predominately lower layers, and thus should provide an interesting contrast to his work. After the observations were begun, it became apparent that one more bit of information might be extracted. The Swan bands of C_2 were sufficiently intense as to allow a determination of the rotational excitation temperature of the chromosphere, a measurement which has not previously been made.

II. Observational techniques

Aside from the interpretation of the results of an investigation like this one, there is also a most formidable observational problem. Hence it seems appropriate to describe the situation, since the better part of four months of observing was necessary to obtain the required spectra.

A cursory glance at the image of the sun as seen at the focus of a solar telescope during the day will show that the seeing is by no means comparable to that which prevails for night stellar observations. However, it has long been known that for a few hours in the earlier part of the morning, immediately after sunrise, the solar seeing is much improved, indeed at its best. Preliminary observations of the flash spectrum showed that under ordinary morning seeing, only a few of the brighter lines were visible. As work progressed, it became apparent that only the very best seeing gave any results at all. More and more plates were exposed, and refinements were added as necessary to take advantage of the good seeing. As a result of the observational program, the following statements may be made.

The seeing on Mount Wilson, where the observations were made, is good enough to obtain useable spectra on approximately 15 mornings per year, all of which occur in the summer months between May and September. With such a dearth of good seeing, it is absolutely necessary to make a successful observation when the conditions permit. The truly high quality of seeing lasts at the most only about 20 minutes, after which the seeing rapidly deteriorates. Since the exposure times necessary are only of the order of 1 to 2 minutes, this might seem like sufficient time to make the necessary observations. However, during

this 20 minutes, the solar telescope underwent considerable changes, which had to be nullified in order to continue observing. For example, if the coelostat mirrors are left exposed to the sunlight for the entire period of good seeing, then the focus of the system is found to change by nearly one meter, an amount which obviously cannot be tolerated even at the long focal length of 150'. Hence during the observations, one must observe briefly, then close the dome of the telescope, and let the mirrors cool. Electric fans were helpful, but introduced such a vibration in the image that they had to be turned off during the exposures. A further complication arises from the fact that when the sun is only a few degrees above the horizon, as it is when the seeing is best, the refraction is changing rapidly, so that the driving clock is no longer accurate. If an observation is made, and the dome closed, say for 3 or 4 minutes, to allow the mirrors to cool, then upon opening the dome one finds that the image has shifted its position considerably, usually by several inches on the 17-inch image. Hence while the mirrors are heating up again, and while the focus is changing, one must stop and carefully put the image tangent to the slit of the spectrograph once again. All this consumes valuable time, and the image has already begun to deteriorate owing to change of focus. All this occurs even though the mirrors of the coelostat are made of Pyrex; perhaps quartz mirrors are to be preferred.

Once these details have been taken care of, the exposure is started, the critical guiding being done by means of a manually tilted plane-parallel glass plate. This plate will keep the image in its proper place for the duration of one exposure, even though the driving clock is not keeping the image stationary. In order to obtain a good exposure,

one must keep the image of the sun within about 1/2 mm of the slit of the spectrograph. The confusion at the sun's limb even in the best seeing is of this order of magnitude, so that it is obvious that some of the light from the limb will go through the slit and contaminate the chromospheric spectrum. Guiding is best done by observing the spectrum visually, with an eyepiece at the end of the plate-holder, while the exposure is going on. By observing some emission lines in this manner, one quickly learns how much encroachment of the limb must be allowed in order to register the nearby chromospheric spectrum. Under the very best seeing, the limb is seen during the exposure only as a rapid series of faint flashes across the width of the spectrum, while the emission lines of the chromosphere stand quite steady.

Because of the few days of good seeing, and the critical conditions, it is desirable to obtain more than one spectrum on each good day. Unfortunately, the 75-foot spectrograph cannot be adjusted to a different wavelength without observing visually the solar spectrum, and identifying the spectral region in that manner. To open the dome of the tower while this was done would spoil the next observation, and so it is best to try several exposures of the same region and pick the best one for photometry. Indeed, this procedure is most necessary, for even after much experience it is impossible to tell before development which of the three or four exposures made will be the best. Besides the perfect seeing and flawless technique required, there still seems to be some element of chance involved.

The chromosphere is known to have only a very faint continuous spectrum, and so it is safe to assume that the continuous background observed on all of the spectra is due to the encroachment of the solar

limb during the exposure. The only way to get rid of this light, it would seem, would be to subtract it off during the reduction of the spectra by photometric means. To do this, one needs a separate spectrum of the very extreme solar limb, in order that this spectrum may be subtracted off, point for point, from the observed spectrum. To get the spectrum of the extreme limb, where the characteristics of the spectrum may be changing rapidly, also requires good seeing, and this observation must be sandwiched in with the rest while the good seeing prevails. Fortunately, it only requires an exposure of about 10 seconds to record the limb spectrum, so that several attempts may be made during a minute or two of good seeing and constant focus.

Throughout these observations, the high dispersion is very useful; however, it also imposes one serious restriction on the observations, that of a fairly small wavelength region. The grating used in the spectrograph was ruled by Babcock, with 400 lines per mm. The blaze of the grating is in the far red in the second order, or in the green of the third order. The linear dispersion on the photographic plate is, then, about 0.53Å/mm in the second order, and about 0.35Å/mm in the third order. Thus in the third order, a total interval of about 270 Å may be observed at one time, since it is possible to fit three 10-inch plates into the plate-holder end to end, at the focus of the spectrograph. One must therefore pay for the high dispersion by making more observations, to cover the spectral regions of interest. The present observations extend from λ5000Å to λ5270Å, and from λ5440Å to λ6570Å. The gap in the interval was due to an oversight in changing orders of the spectrograph. In this particular instance, the blaze of the spectrograph was so strong that the exposure times

were much shorter in the third order green than in the second; hence the use of the higher order was almost mandatory for this region.

Since the main purpose of the observations was to determine line profiles, it was clear that accurate calibrations must be obtained for each plate used. The only equipment available for this purpose at the 150' solar tower consisted of a pair of calibrating slits, one consisting of a set of slits placed end to end and of increasing width, and the other consisting of a single triangular slit. These were to be placed in the position of the ordinary slit of the spectrograph, and the resulting spectrum would appear as a series of spectra of varying density, or as one wide spectrum of varying density, respectively. In the case of the step slit, the width of each step is known, and since the intensity of the light striking the plate is thus known, a calibration of density vs. intensity may be obtained. For the wedge slit, the same calibration is obtained, but is continuous in nature, rather than giving only a few points on the curve.

When these calibrating devices were first used, the spectra were found to be streaked in nature; this was traced to reflections from the objective lens of the telescope. Upon examining the illuminated grating by means of a telescope, several very bright images of various sizes could be seen. When the objective lens was removed from the optical system, these images disappeared, for the most part. The source of a very bright fringe on one side of the grating was never discovered, so this edge of the grating was blocked off with a black paper strip about 1/4 inch in width. The grating still appeared to be unevenly illuminated, however, and so a field lens was inserted just above the slit of the spectrograph and the image of the aperture of the

telescope was projected onto the grating in a uniform manner. This aperture now consisted of a circular opening some 15" in diameter, where the objective lens formerly was placed. This opening itself gave a very rough pinhole image of the sun in the focal plane. In order to make the calibrating exposure of the same approximate time as the chromospheric exposures, it was necessary to move the pinhole image of the sun off axis somewhat, and expose the wedge slit and step slit to the bright sky near the limb of the sun. Each of the calibrating slits came to a very small width at the endpoint, and hence the spectrum lines of the sun were fairly well resolved at one end of the resulting spectrum, and quite blurred out at the other. It is desirable to have a perfectly homogeneous width of spectrum with no absorption lines showing, and hence there was provided a small motor to oscillate the calibrating slits about a pivot at the wide end of the slit, to provide further blurring of the absorption lines. The resulting plates showed a few of the stronger absorption lines as faint wedge-shaped images, but there was always ample area in which the exposed portion of the plate was quite homogeneous for a few centimeters along its length. In making the photometric reductions, this portion of the plate was run on the microdensitometer. A comparison of the calibrations made with the two devices showed that the calibration curves agreed quite closely; therefore the continuous curve was used for the determination of the fundamental calibration curve in each case, and the points resulting from measures of the step slit spectrum were used only as checks.

In cases where accurate photometry is necessary, it is always advisable to have the calibration on the same plate as the exposure to

be calibrated. The size of the plates used for this project did not permit this procedure to be carried out. However, the calibration plates were developed simultaneously with the spectra, and given identical treatment at all times. Throughout, the plates, which were of high contrast and comparatively low speed, were developed for 13 minutes in fresh Eastman D-19 developer, at 68° F. The plates were agitated every 30 seconds throughout this period, and gently wiped with soaked cotton at one minute intervals, in order to reduce any Eberhard effect which may have resulted. Eastman plates were used throughout; IV-F2 plates for the region between λ6000Å and λ6570Å, III-D plates from λ5000Å to λ6000Å, and III-K plates for the region around λ7750Å, where a few exposures were made to record the OI triplet near λ7775Å. In this last case, additional difficulties were encountered, since the eye is no longer sensitive at these wavelengths. Guiding by observing the spectrum was out of the question, therefore, and had to be accomplished by observing the position of the limb of the sun with respect to the slit of the spectrograph, throughout the required 20-minute exposures. Focus changes and deterioration of the seeing were also very troublesome over such a long exposure, but the observations were remarkably successful; on the first try, an excellent plate was obtained, showing the OI triplet in intense emission, with very little continuous background. The success may partially be due to the rather large height in the chromosphere to which these lines are known to extend; they would be more easily recorded without critical guiding than lines which extend only to comparatively low heights.

III. The Observations

In all, some 267 plates were exposed between the dates of May 17, 1951 and October 19, 1951. Of these, about 100 were attempts to obtain chromospheric spectra, while the rest were limb spectra, comparison spectra from the center of the disc, or calibrations. Since there were on the average three exposures of the chromosphere on each of the 100 plates, there were roughly 300 attempts made to record the flash spectrum. Of these 300, only about 25 were at all suitable for photometry, the criterion being the high strength of emission lines and the lack of a great amount of scattered light from the solar limb. The best 15 of these 25 were run on the microdensitometer, the runs being made in both directions, with a slight shift of the plate in between. Since the spectra are about two centimeters in width, and since the central portion of the exposure, where the emission lines are the strongest, is wide compared to the length of the analyzing slit of the microdensitometer, it was possible to obtain two actually different runs from each spectrum. These two runs correspond to very closely the same portion of the chromosphere, and provide additional accuracy when the line profiles are measured. Combining the running speed of the carriage of the microdensitometer with that of the recorder results in a dispersion on the tracings of about 10 cm. per Angstrom, in the second order. The profiles of the emission lines are easily measured on such a scale, by the expedient of overlaying a mm. grid on the chart, and reading off heights of the line as a function of wavelength from the center of the emission.

Before any measures of the profiles can be made, however, it

is necessary to establish the wavelengths, and hence the identities, of the emission features of the spectrum. To accomplish this, the selected plates were measured for wavelengths. One plate only was used in most instances, and two plates in two or three cases.

The comparison lines on the plate were chosen from the stronger absorption lines of the overlying limb spectrum; their wavelengths were taken from the revised Rowland atlas (2) which gives the wavelengths for lines at the center of the disk of the sun. Since the overlying spectrum is that of the extreme limb, it is possible that the wavelengths may be in error by a few thousandths of an Angstrom owing to the "limb shift". However, the derived wavelengths are certainly accurate enough to provide a basis for identification of the element responsible for the line. One additional factor enters into the situation here, however, which is not usually present when determining wavelengths. It must be remembered that the spectrum of the chromosphere and that of the limb are very different in nature, and that the emission lines are superimposed upon a continuous spectrum with absorption lines. When the layers of the photosphere merge into those of the chromosphere, the various absorption lines go into emission in varying degrees. In the chromosphere, lines which were extremely faint in the photosphere are frequently found in strong emission. If there are absorption lines in the neighborhood, due to the overlying limb spectrum, as there often are, then the emission superimposed asymmetrically upon the absorption may result in a substantial shift of the apparent emission peak, and thus, in the measurement of the wavelengths, lead to erroneous values. If the blending is at all heavy, then only an examination of the traces from the limb and from the

chromosphere can separate the effects, and correct the errors. It is of interest to note that in several cases wherein strong lines have been measured for wavelengths and profiles, the subtraction of the superimposed limb spectrum has led to a shift of the center of the emission of the line. In each case, the shift was such that the wavelength agreed more closely with the Rowland wavelength.

A table of the observed emission lines, with their identifications (if known) and wavelengths, is given in the Appendix. The above mentioned wavelength shifts have not been taken into account at all, since comparisons of limb and chromospheric spectra have not been made for each line. A description of the abbreviations used in describing the nature of the emission lines will be found in the introduction to the table.

Identifications have been made from several sources, which are listed in the Appendix. The identification of the carbon lines was accomplished by reference to the work of Johnson (3); this work also provided, after a slight correction, the rotational identifications for all of the C_2 lines observed.

IV. The Level of the Observations

One of the most important pieces of information necessary for any study of the chromosphere is the level of the observations. Conditions change rapidly with height in the chromosphere, and the derived temperatures or turbulent velocities must be given with reference to a given level.

In the present investigation, there is no opportunity to judge the height of the observations from the spectra, as there is in the eclipse observations. In the eclipse observations, the encroachment of the moon's limb can be clearly seen, and the amount of the lower layers of the chromosphere covered by the moon can be determined as a function of time. Thus as the observations progress, before totality, the chromospheric spectra are obtained from higher and higher layers.

Outside of eclipse, however, the level of the observations must be determined from the position of the slit with reference to the limb of the sun. At the 150' solar telescope on Mount Wilson, the diameter of the image of the sun is about 430 mm. From the known diameter of the sun, it follows that 1 mm. on the image corresponds to 3240 km. on the sun. During the observations, the slit was kept at all times within 1/2 mm. of the solar limb. Thus the level of the observations must have been an integration over the chromospheric heights from 0 to about 1600 km. In addition, however, the line of sight of the observations necessarily passes tangentially through all the layers above this, and so there must be contributions from higher layers, but in a smaller proportion owing to the greatly decreased density. Further consideration will be given to this problem in the discussion of the observations of line profiles.

V. The Swan bands of C_2

A conspicuous feature of the chromospheric spectrum outside of an eclipse in the presence of the Swan bands of C_2. The regions near λ5635Å and λ5165Å are crowded with the characteristic molecular bands of this element. The bands are degraded to the violet, the band with its head at λ5165Å (the 0, 0 band) being many times more intense than that with its head at λ 5635Å (the 0, 1 band). Much fainter heads of the nearby higher vibrational bands are also visible, e. g. the (1, 1), (2, 2), and (1, 2) bands. These lines of the fainter bands are just on the limit of visibility on the spectrograms. Wavelengths for them have been determined, when possible, but photometry was possible only in the case of the lines of the (0, 0) and (0, 1) bands. In all, well over 300 lines attributable to the C_2 molecule were measured for wavelengths. Of these, 105 were measured photometrically to determine their intensities. The intensity of each line was taken as its area on the microdensitometer tracing, after appropriate correction from the calibration curve Since this area is necessarily in units of the background spectrum, it is important to consider the intensity variation in that background. The total wavelength interval over which the measured lines extended was about 100Å. In the portion of the spectrum containing the Swan bands, (between 5000 and 5650Å) the continuous energy curve of the sun is near its peak, and therefore is not changing rapidly. Owing to this fact, and the small wavelength interval studied, the variation in the intensity of the background may be neglected.

With the high resolution available, it is obvious that the rotational structure of these bands will be well resolved. Hence a

measurement of the intensities of the individual lines, and the identification of the appropriate rotational quantum number for each line, will allow a determination of the distribution of the molecules over the various rotational levels. From this distribution it is possible to determine a rotational excitation temperature, if it is assumed that the source of the lines exists under conditions of thermal equilibrium, by the use of the Maxwell-Boltzmann distribution law, and the quantum theory.

The thermal distribution of the rotational levels may be found from the product of the Boltzmann factor and the statistical weight of the various states. Each state of an atomic system which has a total angular momentum J actually consists of $2J+1$ levels, which are only separated in the presence of an external field. Since the state with a non-zero value of J will occur with a frequency just $2J+1$ times that of a state with $J = 0$, the factor $2J+1$ is called the statistical weight of the state with the total quantum number J. If we assume for the moment that the molecule is in its lowest vibrational state, then the number of molecules in the rotational level J will be proportional to

$$(2J+1)\,\mathcal{E}^{-\frac{F(J)hc}{kT}} \qquad \ldots\ldots(1)$$

where h is Planck's constant, c is the velocity of light, k is Boltzmann's constant, T is the absolute temperature, and F(J) is the rotational term. This rotational term may be calculated from the expression

$$F(J) = \frac{E_r}{hc} = BJ(J+1) - DJ^2(J+1)^2 \qquad \ldots\ldots(2)$$

where E_r is the rotational energy, h and c are as before, and B and D are the rotational constants for the vibrational state in question. J is again the total angular momentum. For large values of J, the simpler rigid rotator model of the molecule is not sufficiently accurate; the use of F(J) is in eq. (2) comes from a consideration of the non-rigid rotator model. In the present investigation, J-values as high as 72 are encountered, so that the necessity for the use of the more accurate model is obvious. The actual number of molecules in the various rotational states may be found by multiplying the right side of eq. (1) by N, the total number of molecules, and dividing by the sum of the Boltzmann factors over all the states (the partition function). Thus

$$N(J) = \frac{N}{Q_r}(2J+1)\,\mathcal{E}^{-\frac{F(J)hc}{kT}} \qquad \ldots\ldots(3)$$

where Q_r is the partition function. If the transition probabilities were the same for all lines of a band, then the intensity variation of the rotational lines for a given vibrational state would be given by eq. (3). Since this is not in general the case, refinements are required. It may be shown, finally (4) that the intensity of an emission line in a rotation-vibration spectrum for a given electronic transition of the molecule is given by

$$I = \frac{2C\nu^4}{Q_r} S_J\, \mathcal{E}^{-\frac{F(J)hc}{kT}} \qquad \ldots\ldots(4)$$

where ν is the frequency of the line, S_J is the line strength, C is a constant, and the other symbols have their usual meanings. Formulae for the line strengths have been derived on the basis of wave

mechanics, as well as on the old quantum theory, and are given in reference (4), page 208. They depend only on the values of the quantum numbers J and Λ, and hence are easily computed.

If eq. (4) is written in a logarithmic form we have

$$\log_{10} \frac{I}{S_J \nu^4} = \log_{10} \frac{2c}{Q_r} - \frac{F(J)hc}{kT} \log_{10} e \qquad \ldots\ldots(5)$$

Thus it is seen from eq. (5) that by plotting

$$\log_{10} \frac{I}{S_J \nu^4}$$

against

$$F(J)$$

a straight line is obtained, whose slope gives the temperature. That is,

$$\text{slope} = \frac{hc \log_{10} e}{kT} \qquad \ldots\ldots(6)$$

Apart from the usually encountered physical constants, then, one only needs to have the appropriate J value for each line, its frequency, its intensity, and the rotational constants B and D for the vibrational state in question. In the present case, both the bands considered, the (0, 0) and (0, 1) bands, have a common upper vibrational level, and hence the rotational constants are the same in each case. B and D were found from the tables given by Phillips (5) and are found to have the values 1.745 cm.$^{-1}$ and 6.89 x 10^{-6} cm.$^{-1}$

In actual practice, it is best to solve eq. (5) by least squares,

using a slope -intercept form for the equation of the corresponding straight line. The slope thus determined yields the temperature, from eq. (6). From the point of view of molecular spectra, it is not to be expected that the P and R branches, both of which are observed in the Swan bands, will have the same intensities. Certainly the slope of the plot for each branch should be the same, but the individual intensities of the lines will in general be lower by a factor in one of the branches. In this case, the P branch was found to be the more intense. The lines were therefore grouped according to the branch and the J value in the branch. In additional, some use was made of coincident lines in the branches. As the J values increase, the separation of the lines increases; but the lines thus far referred to have not been considered as the triplets which they are known to be. The individual lines of the triplet are well resolved near the head of the band, but as the J value increases, the latter two members of the triplet, usually designated as the P_2 and P_3, etc. lines, slowly merge together, so that for the higher J values the spectrum appears as a series of doublets rather than a series of triplets. Even under laboratory conditions, where the temperatures are much lower, and the lines much sharper, these lines are not resolved. In the sun, lines which are known to be about 0.010A apart are not resolved at all. These coincident lines extend to rather high J values, and would therefore be valuable in obtaining rotational temperatures.

If the assumption is made that these lines have approximately the same separation throughout the spectrum, then it is possible to measure the total intensity of the coincidence, and proceed as before. This scheme has already been used by Miss Adam (6) with good success

in treating the Swan bands as seen on the disc of the sun. It must be emphasized that no attempt is made to predict the intensity of the individual lines making up the coincidence; only the total intensity is measured, as a function of the J value for the pair.

The lines are therefore put into three additional groups, and the final grouping is as follows; (0, 0) band, P_1 and P_2 lines, P_{23} lines, R_1, R_2, and R_3 lines, and R_{23} lines. For the (0, 1) band, P_1 lines, and P_{23} lines were the only two groups. The total of six groups therefore gives six separate determinations of the temperature, and these were found to be in fair agreement, ranging from 3715° K to 5370° K. Two examples of the plots for these lines are shown in (fig. 1) and (fig. 2). Since the (0, 1) band is much the fainter of the two, it is not surprising that the very weak P_1 lines of this band had a very wide scatter of intensities, and being few in number gave the poorest determination of temperature, the 3715° K mentioned above. Hence it was decided to omit these lines from further consideration. When the remaining five determinations are used, the temperature is found to be

$$4610°\,\mathrm{K} \quad \begin{matrix} (\\ (\end{matrix} \begin{matrix} 4210°\,\mathrm{K} \\ 5095°\,\mathrm{K} \end{matrix}$$

where the extreme values correspond to the probable errors in the slope of the determining line.

This value of the temperature is not entirely unexpected. Several investigators, notably Menzel (7), Petrie (8), and Wildt (9), have found excitation temperatures in this general range by several different methods, which include excitation temperatures as derived from the lengths of chromospheric arcs on eclipse spectra, and from intensities of corresponding Fraunhofer and emission lines. In addition several

other determinations of "temperatures" as defined by the methods used to derive them are mentioned by van de Hulst in his review article (11). This rotational excitation temperature also fits in well with the proximity of the level of observation to the solar photosphere, where the excitation temperature is known to lie in the 4000°K - 5000°K range from many measurements. The determination of the excitation temperature by the intensity distribution of rotational lines in molecular spectra is accomplished by means of the assumption that the emitting or absorbing medium is in thermal equilibrium. Although this may certainly not be the case in the solar chromosphere, it at least allows a rough determination of the order of magnitude of the temperature. Following the work of Redman (1) there was much discussion of the high kinetic temperature of 30,000°K as derived by him on the basis of line contours. It now appears fairly certain that his observations lend themselves to a different interpretation, wherein a portion of the motion of the atoms in the line of sight is due to turbulence in the emitting medium. Although the excitation and kinetic temperatures need not be the same except in strict thermodynamic equilibrium, the low excitation temperature found above would indicate a fairly low kinetic temperature, at least much lower than 30,000°K. This matter will be taken up further when the line contours for various elements are considered.

VI. The Measurement of the Line Profiles

Once the microdensitometer tracings had been obtained, it was found that the eye estimates of the intensities of the emission lines were quite misleading. A previous list had been drawn up of lines to be measured for profiles, but this list was revised after inspection of the tracings. Eventually, all of the emission lines which could be reasonably traced to smooth out the "noise" on the tracing due to plate grain were measured for contours, except for a few faint Fe lines. There were more Fe lines than of any other single element, and hence the omission of a few of the poorer ones did not sensibly affect the result.

First of all, the continuum of the tracing was drawn in, using a transparent rule about five feet long. In many instances, the location of the continuum was very difficult to establish, owing to the presence of numerous absorption lines from the overlying limb spectrum. Often the only way of accurately establishing the continuum was by the extension of the background level from nearby, less affected regions. In all cases, the continuum was drawn three times, the endpoints being marked over a short interval, and the mean of the three determinations was taken. The contour of the line was then sketched by overlaying a sheet of tracing paper on the tracing, and drawing a mean line through the original microdensitometer trace. This procedure was repeated twice more, independent tracings being made each time. Finally, the three sketches were superimposed, and a mean trace drawn from them. This was in turn traced back onto the original microdensitometer record, so that the contour could be measured using the clear glass density of the plate as a zero point. The transparent grid was put over the final observed

line contour, and ordinates read off for every millimeter along the trace, out to the point where the line disappeared into the continuum. These ordinates were then converted to intensities by means of the calibration curves, and the emission expressed in units of the background continuum.

Now since the background light also was to be measured, and then subtracted off, the corresponding wavelength interval on the limb spectrum tracings had to be measured. To establish the exact position of the required wavelength region, the following procedure was used. Starting from the center of the emission line, the distance out to several absorption features on either side was carefully measured. Then, on the limb tracing, the absorption lines used as the "anchor points" were located, and the position corresponding to the center of the emission line was determined by measuring back from each line. This resulted in a group of points determining the center of the region to be measured. The points were usually quite close together, not more than two millimeters apart in general. The mean was taken, and the limb spectrum was measured in each direction from this point. Again, the intensities were referred to the continuum.

Since the chromospheric continuous spectrum is known to be very faint, it is sufficiently precise to subtract off all of the background intensity on the chromospheric traces. Since each spectrum had been expressed in terms of the background, a straight subtraction procedure was carried out, resulting in the complete obliteration of the background light outside of the spectral lines.

In the region of the lines, however, the main effect was noticed. In the great majority of cases, the emission line in the chromospheric spectrum was superimposed on an absorption line from the limb

spectrum. Hence it was really more intense than would appear from its height above the continuous background. What is also very important, however, is that its profile was altered greatly by the superposition. The broad chromospheric line was formed on top of a narrower photospheric limb line, and hence the main effect was near the center of the line, where the determination of the half-widths, etc. are made.

There are a few extreme cases wherein this effect is seen to operate in a very spectacular manner. Occasionally, a strong line in the ordinary disk spectrum of the sun will simply disappear, in the observed chromospheric spectrum. Considering the superimposed limb spectrum, however, shows that it simply has gone into emission by an amount just necessary to cancel the absorption of the limb spectrum. If the limb spectrum is subtracted off, then the line appears again. Similarly, if a line is only weakened upon being observed in the chromosphere, then it may be that the line has gone into emission, but not strongly enough to counteract the limb spectrum superimposed upon it. In this case, subtraction of the limb spectrum again will reveal the presence of the line in emission. Thus it appears that a large number of strong lines observed in eclipse spectra, but not in the spectra outside of eclipse, are simply being masked off in this manner. In this investigation no attempt was made to examine all the lines, for this effect, but a few representative lines were examined in detail. One of these is shown in (fig. 3). Here there was no trace of emission in the observed spectrum, but after subtraction an emission line of considerable intensity was seen to appear. Now it is known that many Fraunhofer lines become weaker at the limb, and it is possible that the limb spectrum used in the subtraction technique was not as

close to the limb as was the light which got through the slit during the chromospheric exposure. To test for this effect, the contour may be measured. It turns out that the contours measured in this type of case fit in well with the other chromospheric contours, and not at all with the profiles from limb spectra. Hence in many cases, at least, this effect of superposition may be responsible for the non-appearance of the lines characteristic of the eclipse spectra.

A third case of considerable interest is that when a "double reversal" appears, i. e. when the line as observed in the chromosphere shows emission wings with an absorption core. This may be due to true self-absorption by cooler, higher gases, in some cases, but in the instances examined in this investigation, the subtraction of the limb spectrum resulted in the appearance of a perfectly normal chromospheric emission line, with a contour appropriate to the chromosphere. An example of this type of phenomenon is shown in (fig. 4).

In the remainder of the lines, all conditions intermediate to the three mentioned above were encountered. A few lines of the rare earths had limb lines so faint as to defy detection, and hence required no correction. In other cases, fortunately few in number, the observed profile was actually destroyed by the subtraction process, owing to unsuspected nearby blends of emission lines not strong enough to overcome the superimposed limb spectrum. This subtraction procedure was also carried out in the case of the Swan bands, but here the corrections were very small. The Swan lines were in general so faint that measurement of profiles was not considered practical. A few measures of the most intense lines show that they fit into the general scheme of observations as determined by the other lines.

Once the profiles of the observed lines had been determined, and the subtractions performed, it was necessary to remove the so-called instrumental contour from the results. The instrumental contour was not known for the spectrograph, and hence had to be determined by observation. This is usually done by means of an emission tube of some type, or occasionally by means of an Iodine absorption tube. Early attempts at determining the contour in this manner were not too successful, however, and eventually the atmospheric (telluric) lines of O_2 were used for this purpose. These are the narrowest lines observed in the spectrum of the sun, and a handy group of them occurs near $\lambda 6300\text{Å}$. Thirteen of the best and least blended of these lines were selected from microdensitometer traces of the limb spectrum, and the contours measured with great care. Since these lines are formed at fairly low levels in the earth's atmosphere, their thermal width is very small indeed, and only a small correction on this account is necessary to reduce their contours appropriately, thus obtaining for all practical purposes the profile of the lines as determined purely by the instrument.

The manner in which the instrumental contour is removed from the observed contour is a matter of some importance, in the present case. Very small errors in the half-width of the line will result in large errors in the derived thermal or turbulent velocities. The precise method to use is that of numerical integration of the integral equation describing the combination of two factors distorting the energy distribution of a spectral line. This procedure is very laborious, however, and not worth the effort in the present case. If both of the distorting functions are Gaussian in nature, then the observed and

instrumental half-widths may be disentangled by simple quadratic subtraction. Now one of the distorting functions is known to be Gaussian, i. e. the broadening of the line due to the thermal Doppler motions. However, the instrumental contour is definitely not Gaussian in character, and the Gaussian approximation to that profile may be rather poor. In view of the high dispersion of the observations, and the accuracy of the contours, it seems wise to use some other more accurate method to eliminate the instrumental contour. Such a method, employing Voigt functions, has been outlined by van de Hulst (10) and elaborated on by Elste (12). The Voigt functions arise from the combination of the Gaussian and the dispersion form of the distortion functions, and are characterized by two parameters, β_1 and β_2. β_2 measures the amount of the half-width of the line due to a Gaussian function inherent in the contour, while β_1 measures the amount of the width due to the dispersion function. The disentangling of the various functions is now accomplished by simple or quadratic addition or subtraction of the two parameters for each line; and is therefore quite rapid in practice. The parameters are determined by measurements of the total width at one-half and at one-tenth the maximum intensity of the line. The ratio of these widths is taken, and the parameters found by interpolation in tables of Voigt functions. For a pure Gaussian distortion function, β_1 is zero; for a pure dispersion form, β_2 is zero. Thus by examining the parameters, it may be seen what sort of a composition of the two types of functions is determining the shape of the given line.

From the measurements of the O_2 lines, the parameters

$$\beta_1 = 0.01807$$
$$\beta_2^2 = 0.001819 \qquad \text{(in the second order)}$$

are found, for λ6300Å. These may be modified for use at other wavelengths by multiplying them by

$$\frac{\lambda}{6300} \quad \text{and} \quad \left(\frac{\lambda}{6300}\right)^2 \quad \text{respectively}$$

Extension to the third order, where some of the observations were made, may be accomplished by considering the angular half-widths of the spectrum lines as formed by the grating, and the linear dispersion as they change from order to order. The appropriate factor is 0.696. Therefore

$$\beta_1 = 0.01258$$

$$\beta_2^2 = 0.000881 \qquad \text{(third order)}$$

and extension to other wavelengths than λ6300Å can be made as before.

In making the correction for the instrumental profiles, it is found in the present investigation that about one-half of the lines will not admit to this treatment. That is, they may have abnormal widths at either of the index points, and not fit into the Voigt tables, or they may yield impossible values in later stages. This is probably due to the occurrence of blends in the wings of lines, or of absorption features affecting the subtraction technique. In order to gain some use of the lines which could not be reduced in the Voigt method, the correction was made in those cases by the usual Gaussian quadratic subtraction. It is interesting to note that there were systematic differences in the widths determined from the two methods, where elements of different atomic weight were compared; i.e. the Voigt method yielded consistently smaller line widths than the Gaussian method. The Voigt method is the more accurate of the two, and hence the method should be used

when possible.

Omitting the very faint lines, and omitting badly blended lines, it was found possible to obtain 214 individual measures of line contours. Among these lines are elements ranging in atomic weight from 4 (Helium) to 157 (Gadolinium); the wide spread in atomic weights is particularly useful in the interpretation of the observed contours.

VII. The Observed Profiles and their Interpretation.

Once the procedure just described had been carried out on all the observed lines, it was immediately evident that the final contours were not Gaussian in nature. Owing to blends and the resulting uncertainty of the width of the line near the continuum, the parameters show a considerable scatter. However, even the strong lines, whose parameters are much more certain, nearly always show a finite value for the parameter β_1, and thus are not Gaussian in profile. The following table contains the wavelengths of the observed lines, the identification, the derived Voigt parameters (corrected for instrumental contour), the resulting total halfwidth, and finally two factors used in later discussion of the profiles. These final two factors are simply the total halfwidth and the Gaussian Voigt parameter, corrected for wavelength of the individual line.

TABLE I

λ	ELEMENT	β_1	β_2^2	h(Å)	$\frac{h}{\lambda}$ ($\times 10^5$)	$\frac{\beta_2^2}{\lambda^2}$ ($\times 10^{10}$)	REMARKS
5875	He I	.0998	.05187	.497	8.460	15.02	
		.1413	.03132	.458	7.796	9.08	
5577.359	[OI]?			.086	1.542		
				.119	2.134		
7771.950	OI	.0992	.007328	.276	3.551	1.213	
		.0927	.007389	.266	3.422	1.223	
7774.177	OI	.0941	.007628	.270	3.473	1.262	
		.0869	.012039	.293	3.769	1.991	
7775.397	OI	.0963	.003034	.230	2.958	.484	
		.0818	.006676	.243	3.125	1.104	

λ	ELEMENT	β_1	β_2^2	h(Å)	$\frac{h}{\lambda}$ ($\times 10^5$)	$\frac{\beta_2^2}{\lambda^2}$ ($\times 10^{10}$)	REMARKS
6347.109	Si II			.141	2.222		
		.0132	.004081	.121	1.906	1.013	
6371.375	Si II	.0212	.002326	.104	1.632	.549	
		.0253	.002109	.107	1.679	.519	
6210.667	Sc I	.0316	.000027	.125	2.012	.00701	
		.0000	.003068	.092	1.481	.795	
5062.109	Ti I	.0211	.000251	.055	1.086	.098	
		.0206	.000078	.046	.908	.030	
5226.547	Ti I	.0126	.007494	.158	3.023	2.744	POOR
				.175	3.348		
5490.716	Ti II (?)			.091	1.658		
		.0084	.001909	.082	1.493	.633	
5644.147	Ti I	.0227	.003550	.126	2.232	1.114	POOR
		.0230	.004590	.139	2.463	1.398	POOR
5648.568	Ti I			.098	1.735		
				.094	1.664		
5662.157	Ti I			.079	1.395		
				.078	1.378		
5702.668	Ti I			.031	.543		
		.0000	.001181	.056	.982	.342	
5762.300	Ti I	.0000	.003540	.099	1.718	1.066	
				.110	1.909		
5766.331	Ti I			.050	.868		
		.0071	.001837	.081	1.405	.552	
5774.040	Ti I	.0023	.000328	.033	.572	.098	

λ	ELEMENT	β_1	β_2^2	h(Å)	$\frac{h}{\lambda}$ ($\times 10^5$)	$\frac{\beta_2^2}{\lambda^2}$ ($\times 10^{10}$)	REMARKS
		.0047	.000070	.019	.329	.021	
5785.987	Ti I	.0180	.001079	.076	1.314	.322	
		.0104	.002288	.091	1.572	.783	
5804.255	Ti I			.093	1.602		
				.096	1.654		
6220.469	Ti I	.0047	.001746	.075	1.206	.451	
		.0164	.000374	.053	.852	.097	
6081.448	V I			.065	1.069		
				.073	1.200		
6090.212	V I	.0021	.003097	.095	1.560	.835	
		.0000	.003153	.093	1.527	.850	
6119.533	V I	.0147	.001250	.076	1.242	.334	
		.0111	.002038	.086	1.405	.520	
6199.199	V I			.118	1.903		
				.116	1.871		
6243.106	V I	.0021	.004325	.111	1.778	1.109	POOR
				.128	2.050		
6242.822	V I			.115	1.842		
				.112	1.794		
6251.821	V I	.0053	.002739	.091	1.456	.674	
		.0014	.003237	.091	1.536	.828	
6285.177	V I	.0049	.000958	.057	.906	.242	
				.071	1.130		
6296.499	V I	.0313	.000681	.086	1.366	.172	
		.0370	.000030	.075	1.191	.007	

λ	ELEMENT	β_1	β_2^2	h(Å)	$\frac{h}{\lambda}$ ($\times 10^5$)	$\frac{\beta_2^2}{\lambda^2}$ ($\times 10^{10}$)	REMARKS
5214.136	Cr I			.080	1.534		
				.068	1.304		
5783.059	Cr I	.0204	.000564	.066	1.141	.168	
		.0220	.000430	.064	1.107	.224	
5783.863	Cr I	.0131	.001933	.088	1.521	.578	
		.0179	.001736	.090	1.556	.519	
5787.913	Cr I	.0077	.003402	.106	1.831	1.016	
		.0053	.003935	.110	1.900	1.1748	
5100.660	Fe II	.0174	.001298	.081	1.588	.499	
		.0168	.001023	.073	1.431	.393	
5132.683	Fe II	.0233	.001369	.090	1.753	.520	
		.0107	.002849	.099	1.929	1.041	
5197.578	Fe II	.0014	.007428	.145	2.789	2.750	POOR
		.0111	.006422	.146	2.809	2.378	POOR
5234.632	Fe II	.0066	.007619	.152	2.904	2.781	POOR
		.0069	.007912	.159	3.038	2.888	POOR
5256.937	Fe II			.092	1.750		
		.0033	.002336	.084	1.568	.845	
5259.742	Fe II			.057	1.084		
				.067	1.274		
5264.810	Fe II			.102	1.937		
		.0075	.002913	.105	1.994	1.051	
5525.556	Fe I			.100	1.810		
				.100	1.810		
5534.858	Fe II			.114	2.059		
				.075	1.355		

λ	ELEMENT	β_1	β_2^2	h(Å)	$\frac{h}{\lambda}$ ($\times 10^{-5}$)	$\frac{\beta_2^2}{\lambda^2}$ ($\times 10^{10}$)	REMARKS
5627.499	Fe II			.087	1.546		
				.098	1.742		
5732.718	Fe II			.148	2.582		
6084.107	Fe II			.073	1.200		
				.089	1.463		
6129.708	Fe II			.090	1.468		
				.075	1.223		
6238.386	Fe II	.0144	.001677	.085	1.362		
		.0159	.001040	.073	1.170		
6239.357	Fe II			.075	1.202		
				.075	1.202		
6239.944	Fe II	.0116	.001736	.062	.994	.446	
		.0266	.000486	.073	1.170	.125	
6247.559	Fe II	.0039	.003671	.105	1.680	1.115	
		.0082	.003554	.108	1.728	.911	
6369.460	Fe II	.0154	.000352	.051	.801	.088	
		.0062	.001483	.071	1.115	.365	
6416.924	Fe I	.0152	.000318	.049	.764	.077	
		.0180	.002240	.100	1.558	.544	
6432.690	Fe II	.0298	.000177	.067	1.042	.043	
		.0015	.002708	.088	1.368	.654	
6456.391	Fe II	.0159	.001715	.087	1.348	.411	
		.0157	.001960	.092	1.425	.470	
6516.091	Fe II	.0093	.002766	.098	1.504	.651	
				.117	1.800		
6086.680	Co I	.0250	.001601	.097	1.594	.432	POOR

λ	ELEMENT	β_1	β_2^2	h(Å)	$\frac{h}{\lambda}$ ($\times 10^5$)	$\frac{\beta_2^2}{\lambda^2}$ ($\times 10^{10}$)	REMARKS
		.0399	.000706	.100	1.643	.190	POOR
6257.574	Co I			.098	1.566		
				.073	1.167		
6271.489	Co I	.0018	.001255	.061	.973	.319	POOR
				.101	1.610		
6347.852	Co I	.0106	.000389	.045	.709	.096	POOR
				.059	.929		
5592.156	Ni I	.0082	.002906	.099	1.770	.929	BLEND
				.061	1.091		BLEND
5592	Ni I	.0109	.002958	.103	1.841	.946	BLEND
		.0184	.001962	.095	1.698	.627	BLEND
5614.781	Ni I			.121	2.155		
				.123	2.191		
5625.315	Ni I	.0160	.001392	.081	1.440	.440	
				.098	1.742		
5694.990	Ni I			.096	1.686		
				.084	1.401		
5805.212	Ni I	.0000	.002744	.087	1.499	.833	
		.0024	.003001	.094	1.619	.890	
6086.287	Ni I	.0035	.003845	.107	1.758	1.035	POOR
		.0169	.002226	.098	1.610	.601	
6183.898	Ni I	.0061	.001652	.074	1.197	432	
				.105	1.698		
5473.384	Y II			.107	1.955		
				.100	1.827		
5521.583	Y II			.067	1.214		

λ	ELEMENT	β_1	β_2^2	h(Å)	$\frac{h}{\lambda}$ ($\times 10^5$)	$\frac{\beta_2^2}{\lambda^2}$ ($\times 10^{10}$)	REMARKS
		.0018	.001496	.066	1.195	.491	
5544.627	Y II			.075	1.353		
				.081	1.461		
5112.280	ZrII			.066	1.291		
				.070	1.369		
5191.606	ZrII			.132	2.542		
		.0078	.003549	.108	2.080	1.316	POOR
6114.799	ZrII	.0164	.000045	.036	.694	.012	POOR
				.069	1.128		
5769.077	La II	.0181	.001101	.077	1.334	.331	
		.0111	.001194	.070	1.213	.358	
5805.768	La II			.065	1.120		
				.080	1.378		
5863.718	La II	.0014	.001027	.055	.938	.299	
				.069	1.177		
6320.401	La II	.0087	.002503	.093	1.472	.627	
				.102	1.614		
6390.489	La II	.0041	.000116	.023	.360	.028	
				.068	1.064		
5117.179	Ce II	.0091	.000450	.046	.899	.172	
		.0042	.000509	.046	.899	.195	
5187.459	Ce II	.0024	.001094	.058	1.118	.407	
		.0055	.000903	.056	1.080	.335	
5200.133	Ce II (?)			.116	2.230		Cr ??
				.113	2.173		Cr ??

λ	ELEMENT	β_1	β_2^2	h(Å)	$\frac{h}{\lambda}$ ($\times 10^{-5}$)	$\frac{\beta_2^2}{\lambda^2}$ ($\times 10^{-10}$)	REMARKS
5468.381	Ce II			.120	2.194		BLENDED
				.108	1.975		BLENDED
5472.304	Ce II			.072	1.316		
				.074	1.352		
5512.074	Ce II			.133	2.412		
				.125	2.267		
				.062	1.105		
5610.242	Ce II			.059	1.052		
		.0139	.001020	.070	1.210	.306	
5768.879	Ce II			.053	.92		
6033.569	Ce II			.057	.945		
				.104	1.724		
6034.213	Ce II	.0134	.000179	.040	.663	.049	POOR
		.0176	.000170	.046	.762	.047	POOR
6043.393	Ce II			.042	.695		POOR
		.0025	.000275	.030	.496	.075	POOR
6043.387	Ce II	.0015	.000346	.033	.546	.095	POOR - same line as previous one. different plate.
				.047	.778		
6272.030	Ce (?)			.031	.494		
5089.852	Nd			.070	1.375		
				.066	1.297		
5130.598	Nd	.0175	.000442	.057	1.111	.168	
		.0150	.001440	.074	1.442	.433	
5192.622	Nd	.0042	.001843	.076	1.464	.684	POOR
		.0040	.001804	.075	1.444	.669	POOR
5449.586	Nd II			.083	1.581		

λ	ELEMENT	β_1	β_2^2	h(Å)	$\frac{h}{\lambda}$ ($\times 10^{-5}$)	$\frac{\beta_2^2}{\lambda^2}$ ($\times 10^{-10}$)	REMARKS
		.0286	.000172	.065	1.238	.062	
5255.524	Nd II	.0022	.001847	.074	1.408	.670	
		.0062	.001332	.068	1.294	.482	
5451.143	Nd II			.074	1.358		
				.084	1.541		
5485.722	Nd II			.089	1.662		
				.074	1.349		
5688.531	Nd II			.104	1.828		
		.0177	.000943	.073	1.283	.291	
5740.864	Nd			.090	1.568		
				.079	1.376		
5742.096	Nd			.086	1.498		
				.066	1.149		
5744.746	Nd			.117	2.036		POOR
5842.382	Nd II			.074	1.267		
				.057	.890		
5842.382	Nd II			.081	1.411		same line as previous one.
				.106	1.814		different plate.
5106.608	Sm (?)	.0156	.001263	.078	1.527		BLENDED
				.081	1.586		
6299.621	Sm	.0072	.002914	.108	1.714		POOR
				.098	1.556		
5011.754	Gd ?	.0192	.000396	.058	1.157		POOR

Several courses of action are now open, in order to interpret the observed profiles. We shall therefore proceed to make several assumptions, and

find the one which gives the most reasonable interpretation of the contours.

1). We may assume that the total width of the line is due to thermal Doppler motions, and that the wings of the line are due to observational errors. This assumption is admittedly naive, since the observed contours are not likely to be so far in error.

The relation between the temperature of the emitting medium and the width of the resulting spectrum line may be found in the following manner. If the distribution of the velocities of the atoms is assumed to be Maxwellian, then the number of atoms moving in the line of sight with velocities between v and v + dv is given by the expression

$$d N(v) = \frac{N}{\alpha \sqrt{\pi}} \varepsilon^{-\frac{v^2}{\alpha^2}} dv \qquad \ldots\ldots(7)$$

where α , the most probable speed, is given by

$$\frac{1}{2} M \alpha^2 = K T \qquad \ldots\ldots(8)$$

and where M is the mass of the atom in question, and T is the temperature of the medium. Thus it is seen that the velocity distribution is a curve of the Gaussian type. We assume that there are not other broadening effects present, and it is then possible to derive a relation between the most probable velocity of the atoms and the observed halfwidth of the spectrum line. The halfwidth is defined as the full width of the line at the point where the intensity has fallen to one-half its

maximum value. Doppler's principle states that

$$\frac{\Delta\lambda}{\lambda} = \frac{v}{c} \quad \text{or} \quad dv = \frac{c\,d\lambda}{\lambda} \qquad \ldots\ldots(9)$$

The intensity distribution within the spectral line is proportional to the number of atoms radiating at a given wavelength, if there are not other broadening effects acting. Thus combining (9) with (7), we have

$$I(\lambda)\,d\lambda = \frac{c\,I_o}{\lambda\alpha\sqrt{\pi}}\,\varepsilon^{-\frac{c^2(\lambda-\lambda_o)^2}{\alpha^2\lambda_o^2}}\,d\lambda \qquad \ldots\ldots(10)$$

Here $I(\lambda)$ is the intensity of the line at wavelength λ, c is the velocity of light, I_o is the total intensity of the line, λ_o is the wavelength at the center of the line, and α is the most probable velocity. The factor in front of the exponential may be taken as the central intensity of the line: then the exponential factor shows how the intensity varies with wavelength in terms of this central intensity. We are interested in the width of the curve at the point where the intensity has fallen to one-half its central value. At this point, then,

$$\varepsilon^{-\frac{c^2(\lambda-\lambda_o)^2}{\alpha^2\lambda_o^2}} = \frac{1}{2} \qquad \ldots\ldots(11)$$

and the total halfwidth of the line is given by

$$h = \frac{2\alpha\lambda}{c}\sqrt{\log_e 2} \qquad \ldots\ldots(12)$$

From eq. (8), we can find the temperature, having solved eq. (12) for the velocity. That is,

$$T = 60.2 \mu \alpha^2$$

.....(13)

where μ is now the atomic weight.

From the two Voigt parameters, the profile of the line may be reconstructed, and the total resulting halfwidth derived. This is the value in column 5 of Table I. Even though the line widths derived by simple quadratic addition are systematically higher, we may use the lines which were not treated by the Voigt profile method without losing much accuracy. Then, using all the values for the halfwidth, as given in Table I, we use eq. (12) to compute the thermal velocities. The values of $\frac{h}{\lambda}$ given in column 6 of the table are therefore averaged by elements, the computations carried out, and the following results obtained. (First three columns).

TABLE II

Element	α, km./sec.	Temperature, °K (no turbulence)	Temperature, °K (with turbulence)
He	14.6	51,500	50,500
O	6.1	35,600	32,100
Si	3.3	18,800	12,900
Sc	3.1	26,800	17,100
Ti	2.7	20,800	10,500
V	2.7	22,000	11,100
Cr	2.7	22,300	11,100
Fe	2.9	29,600	16,200
Co	2.3	18,600	5,900
Ni	3.0	30,900	18,400
Y	2.7	39,000	19,900
Zr	2.7	41,000	21,100
La	2.1	36,800	7,030
Ce	2.0	32,000	1,950
Nd	2.5	55,000	48,200

As is seen from the third column, the temperatures range from roughly

20,000 to 50,000°K. This is the general range of values found by Redman (1), who interpreted the widths of his lines in this manner. However, this interpretation has been criticized by Unsold (13), who explained the heavy-element profiles of Redman in a different manner. In addition, the model of the chromosphere with these high temperatures has met several strong objections, (cf. van de Hulst, (11)). A refinement which was considered, but rejected, by Redman, and which has been elaborated by Unsold (13), is the consideration of turbulence. If the medium is assumed to be in a state of turbulent motion, and if the turbulent elements are assumed to have a Gaussian distribution of velocities, then the turbulent velocities can be subtracted quadratically from the velocities corresponding to the total observed width, and since the thermal part of the velocity is thereby reduced, a lower temperature will result. Now the measures of the rare earth elements are considered to be reasonably good, even though the lines are in general faint. These elements have the smallest line widths, and hence the smallest velocities. If we average the last few elements (La, Nd and Ce) as to velocity and molecular weight, and then subtract off, quadratically, the amount of velocity due to a thermal distribution corresponding to a temperature of about 4600°K, we obtain the largest value that the turbulence can have, and still leave these elements with reasonable thermal widths. The temperature 4600°K is chosen, since it is near the boundary temperature of the sun, and is typical of the excitation temperatures found for chromospheric lines by other means. When this procedure is carried out, it is found that the maximum turbulent velocity assignable on this basis is

$$\alpha_{(TURB.)} = 1.89 \text{ Km./sec.}$$

If this amount of turbulence is subtracted off, quadratically, and the temperatures computed on the basis of the residual thermal velocities, we find the temperatures given in column 4 of Table II. It is seen that the temperatures for the heavier elements are substantially reduced, but that they are still very high in comparison with the temperatures near the boundary of the sun. It is thus apparent that the assumption 1) is a rather poor one, and leaves a considerable temperature variation, in addition to the high value of the temperature. We therefore refine the concepts further, as follows.

> 2). Second Assumption. We assume that the total width of the profiles is the incorrect parameter to use. We further assume that only the Gaussian portion of the profile is due to the temperature, and that the rest of the width is due to some other effect.

The amount of the width of the profile which is due to the two different types of broadening function is conveniently given by the two Voigt parameters. In accordance with our second assumption, we now take only the Gaussian portion of the width, and compute temperatures with it. The sixth column of Table I gives the appropriate values to use. These factors are now examined in the light of the observed contours. The "Remarks" column gives an indication of bad blending, uncertain wings, and other causes which conspire to make the values of the Voigt parameters incorrect. We now choose only the best lines, and omit all those lines which are marked as poor or blended, and omit all lines, of course, which could not be reduced according to the Voigt profile method. The results are given in Table III.

TABLE III

Element	α, km./sec	Temperature, °K (no turbulence)	Temperature, °K (with turbulence)
He	10.40	26,050	25,480
O	3.30	10,500	8,200
Si	2.50	10,500	6,500
Sc	1.90	9,770	3,300(1)
Ti	1.87	10,120	3,260(3)
V	2.11	13,600	6,350(3)
Cr	2.34	17,232	9,770(2)
Fe	2.34	15,870	10,520(2)
Ni	2.39	20,200	11,800(1)
Y	2.10	23,600	10,870(1)
La	1.71	24,600	4,680(3)
Ce	1.65	22,950	2,870(2)
Nd	1.77	27,370	6,690(3)

The temperatures in the third column are again rather high, but seem more consistent and homogeneous than before. The temperature for He is still very high, but that is to be expected; this line shows odd behavior, extending to great heights in the chromosphere.

We may again refine the plan of attack, as we did before. If we assume now that part of the Gaussian width of the curves is due to turbulence, and average over the last three elements for velocities and atomic weights, then we can again remove as much turbulent velocity as will leave a sufficient width to account for a low temperature of about 4600°K for the rare-earth lines. Carrying out this procedure as before, we find that we can now subtract off a turbulent velocity of

$$\alpha_{(TURB)} = 1.54 \text{ km./sec.}$$

which is not substantially different from the value used under the first assumption. The resulting temperatures are given in the last column of Table III, together with their weights as determined from the number and quality of the lines used for the calculation. The situation is

seen to be much improved, now, with only a few values above 10,000°K. Excluding the first three lines, which are peculiar because of their high excitation potential, the weighted mean of the temperatures is

$$T = 6440°K.$$

Thus on our second assumption, the Gaussian part of the curve, with some turbulence removed, yields a fairly low value for the temperature.

The situation is still unsatisfactory, however, since we have neglected the portion of the width of the line due to the finite value of the parameter β_1.

If some interpretation of this remaining width can be found, then the low value for the temperature will be justified. We therefore look for some broadening effect which has a dispersion-like distribution function across the spectral line. Two sources immediately suggest themselves; collisional broadening and the Stark effect. The first of these is very unlikely to account for the amount of broadening observed, owing to the low densities and pressures in the chromosphere. The second effect has been considered by Redman (1), and shown to be very small even for Hydrogen. The effect is much smaller on Helium, and tremendously much smaller for the other elements. Thus these two possibilities must be abandoned.

There seems to be only one remaining possibility; that the observed contours are due to the integration along the line of sight over the higher and lower layers of the chromosphere. Thus a temperature gradient, or a change in turbulent velocity with height, might cause the observed line profiles. We therefore examine this hypothesis.

3). Third Assumption. The observed contours are due to the integration along the line of sight over various layers of the chromosphere.

To test this assumption, we must assume some model for the chromosphere. Such a model is given by van de Hulst (11), and is derived on the basis of observed gradients, and with a minimum of theoretical assumptions. An important feature of this model is the very small temperature gradient; the temperature at the bottom of the chromosphere is taken as 4600°K, and rises only to about 6500°K in 6000 km. On this model, therefore, the profiles may not be explained as the sum of many profiles, each formed at a different temperature level in the chromosphere. Since the line width varies as the square root of the temperature, the small gradient is not very effective in changing the width of the line with height. Since the line widths are nearly all the same, the Gaussian curves add to produce a near-Gaussian curve of the same approximate width, and this is contrary to the observations. The only remaining possibility then is to attribute a different turbulent velocity to each level of the chromosphere. We therefore postulate a chromosphere with a low temperature gradient, but with a large increase of turbulent velocities with height.

We shall now proceed to show that the model of the chromosphere as given by van de Hulst explains the contours of the observed lines, if the turbulence is assumed to increase with height. Using van de Hulst's model, one may compute the density variation with height. For a given line, and with the temperature given by the model, one can also compute the relative numbers of atoms excited to a sufficient degree to emit the line in question. The product of these two factors gives the favorability of emission as a function of height. Since the density variation is the same for all elements, it is seen that the

variable of importance in comparing various lines is the excitation potential, which enters through the Boltzmann factor. The following table compares the favorability for emission of lines of three excitation potentials; 4 volts, 11 volts, and 21 volts. These potentials are characteristic of the lines of the rare earths and metals, Silicon and Oxygen, and of Helium, respectively, which were observed in the present work.

TABLE IV

Height, km.	T	Total density	Density Variation	f(21)	f(11)	f(4)
0	4600	16.0		0	0	0
250	4800	15.3	-0.70	0.27	-0.19	-0.52
500	4950	14.6	-1.40	0.24	-0.54	-1.09
750	5100	14.0	-2.00	0.28	-0.81	-1.57
1000	5300	13.4	-2.60	0.45	-1.00	-2.02
1500	5600	12.4	-3.60	0.52	-1.44	-2.82
2000	5850	11.5	-4.50	0.44	-1.91	-3.56
3000	6000	10.9	-5.10	0.28	-2.28	-4.08
4000	6100	10.5	-5.50	0.17	-2.52	-4.42
5000	6300	10.1	-5.90	0.32	-2.64	-4.72
6000	6500	10.5	-6.10	0.65	-2.56	-4.82

In the table, all but the first two columns are given as exponents of powers of ten. The f's are the favorability factors, with the pertinent excitation potentials in parenthesis. It is evident from examining the last three columns, that lines of high excitation potential may be expected to extend to greater heights in the chromosphere than those with low excitation potential. In the present work, lines of both types are included, and the lines of higher potential are those from HeI, OI, and SiII. These lines are known to extend to great heights in the chromosphere, from eclipse observations; for example, the He I line at $\lambda 5875\text{Å}$ has an eclipse height of 7500 km., while the heights for the three lines of the infrared oxygen triplet are given as 6000 km.

The heights of the lines seem reasonable, upon looking at the f's in the table. For He, the conditions for excitation remain favorable throughout the extent of the table. For O, the conditions get poorer at a moderate rate, and for the lines of low excitation potential, such as the rare earths and metals, the conditions become less favorable with height at a rapid rate. The rare-earth lines usually have heights, according to the eclipse observations, of the order of 500 km.

Now to examine the hypothesis of an increase of turbulence with height, we must have very accurate profiles. For this reason, the profiles of the Oxygen triplet in the infrared will be used as a test. They are the most accurately determined of all the measured profiles. From six determinations of the Voigt parameters of these lines, we find

$$\beta_1 = 0.0918$$
$$\beta_2^2 = 0.00735$$

The problem is to see if it is possible to produce a profile of these parameters by adding the contribution of lines from various levels in the chromosphere. From an examination of Table IV, and the f factor for OI, it seems reasonable to assume a thermal distribution of velocities corresponding to a temperature of 5000°K. Because of the very slow variation of temperature with height, we will use this temperature at all heights, with very little error.

The technique used is to assume a turbulent velocity for each height in the chromosphere. Assuming the distribution of turbulent velocities is Gaussian, the square of this velocity is then added to the square of the thermal velocity. The intensity of the line at each level is taken to be proportional to the factor, f. Thus the lines at higher levels have less weight in the determination than do those formed at

lower levels. Curvature of the layers is neglected, as it is not important for a rough approximation such as the present one. In addition, since the contributions of the higher levels is rather small, according to the f factor, only the levels up to and including the 1000 km. level will be considered.

A trial and error method was used for finding the turbulent velocities. The contours of the lines at the various levels were found from the Gaussian distribution function; the lines were plotted to scale according to the f factor for the level, and the curves added ordinate by ordinate. Although this process does not converge rapidly, it was found after several attempts that the profile of the OI lines could be reproduced to within the errors in the determination of the Voigt parameters for them, by the following distribution of turbulent velocities with height.

TABLE V

Height, km.	Turbulent Velocity, km./sec.
0	3.5
250	7.0
500	10.0
750	12.0
1000	14.0

These values must be considered only as a fair approximation, since the contribution of the higher levels was omitted.

Thus it is seen that the contours of the Oxygen lines have been reproduced by assuming a low temperature for the chromosphere, and with the above turbulent velocities as a function of height. Therefore it seems that the temperature of the chromosphere, in the 0 - 1500 km. region, must be in the neighborhood of 5000°K to 6000°K, which is fairly close to the boundary temperature of the sun.

Now under our second assumption, above, we found that the widths of the elements as a function of atomic weight fall in fairly well with such a scheme. We there took out a low thermal velocity, and found that the remaining width was due to a non-Gaussian curve. The non-Gaussian part has been interpreted as the sum of a series of Gaussian curves each resulting from a different level. Though this was successfully done for the accurately known profiles of the Oxygen lines, there is one bit of evidence which might seem somewhat embarrassing at this point. The turbulent velocities found in the case of Oxygen for the zero level of height (i.e. 3.5 km./sec.) are so large that they more than account for the total width of the lines of the heavier elements, as found under assumption 1). This seeming paradox may be traced to the observational procedure, however.

As has been pointed out, the OI lines are of great height in the chromosphere, and the gradient of the f values for them is rather low, in comparison to that for the metals and rare-earths. When the observations are made, the slit is kept within 1/2 mm. of the limb of the sun; that is, the height of the observations is thus kept below about 1600 km. However, the rare earth and metallic lines are known from eclipse observations to extend only to very low heights, of the order of 300 to 700 km. Thus during the exposure, these lines will not be seen unless the slit occasionally dips close to the limb, where these lines are seen in emission. The Oxygen lines, on the other hand, are seen everywhere throughout the region of observation. Thus they will be recorded with good density without going so close to the limb. Essentially, then, the zero point of height for the Oxygen lines is higher in the chromosphere than that for the rare earths and metals.

When the heavy-element lines are observed, the integration over heights in the chromosphere is much smaller than when the oxygen lines are observed. Thus the zero-point for the Oxygen lines may actually be an integration over the lower portion of the chromosphere; the value of 3.5 km./sec. for the turbulence at the lowest level, therefore, is actually an integration over the lower layers, and the true value of turbulent velocity for the lower levels of the heavy-element lines will indeed then be smaller than this value.

Similarly, the large turbulent velocities found for the Oxygen lines at heights of 500, 750, and 1000 km. need not affect the widths of the heavy-element lines to any large extent; the lines of those elements are so faint by the time they reach these heights, that the contribution from the higher levels is negligible.

It is possible, also, that a great portion of the width of the Helium line could be explained in this way, however, this line has been left out of consideration from this point of view owing to the possibility of superexcitation of the line by back radiation from the corona.

The profiles of the heavy-element lines might be tested in a similar manner to the Oxygen line profiles; however, these lines are much fainter, and the limb-correction is much larger. Therefore it is felt that a definitive determination of the turbulence as a function of height would not be possible using these lines. However, it must be emphasized that their non-Gaussian contours may be explained in the same manner as the OI lines.

Although it is not the work of the present thesis to present a theory of the chromosphere, it may be mentioned that the turbulent

velocities may be expected for several reasons. The presence of short-lived, high velocity jets in the chromosphere, as well as the underlying granulation of the photosphere, suggest that a state of turbulent motion exists. In addition, theories of heating and support of the chromosphere incorporating pressure waves or shock waves, or mass motions of the gases, all are suggestive of the existence of turbulence. It is of interest to note, also, that in a recent paper Unsold (13) in combining several sources of information as to turbulent velocities, finds a velocity of 9.6 km./sec. at zero height, and a velocity of 15 km./sec. at 1000 km. The Oxygen line contours in the present work do not admit to interpretation on the basis of these velocities.

VIII. References

(1) R. O. Redman, Monthly Notices of the Royal Astronomical Society, (1942), 102, p. 140.

(2) St. John and others, Revision of Rowland's Preliminary Table of Solar Wave-lengths, (1928).

(3) R. C. Johnson, Philosophical Transactions, (1927), 226, p. 157.

(4) G. Herzberg, Spectra of Diatomic Molecules, 2nd Ed., 1950, D. van Nostrand.

(5) J. G. Phillips, Astrophysical Journal, (1948), 108, p. 434.

(6) M. G. Adam, Monthly Notices of the Royal Astronomical Society, (1938), 98, p. 544.

(7) D. H. Menzel, Publications of the Lick Observatory, (1931), 17, Part 1.

(8) W. Petrie, Journal of the Royal Astronomical Society of Canada, (1944), 38, p. 117.

(9) R. Wildt, Astrophysical Journal, (1947), 105, p. 36.

(10) H. C. van de Hulst and J. J. M. Reesinck, Astrophysical Journal, (1947), 106, p. 121.

(11) H. C. van de Hulst, in The Sun, ed. by G. Kuiper, (1953), University of Chicago Press, Chapter 5.

(12) G. Elste, Zeitschrift fur Astrophysik, (1953), 33, p. 39.

(13) A. Unsold, Zeitschrift fur Naturforschung, (1952), 77, p. 121.

(14) Charlotte E. Moore, A Multiplet Table of Astrophysical Interest, revised edition, (1945) Contributions of the Princeton University Observatory No. 20.

(15) Massachusetts Institute of Technology; Wavelength Tables, (1939), John Wiley.

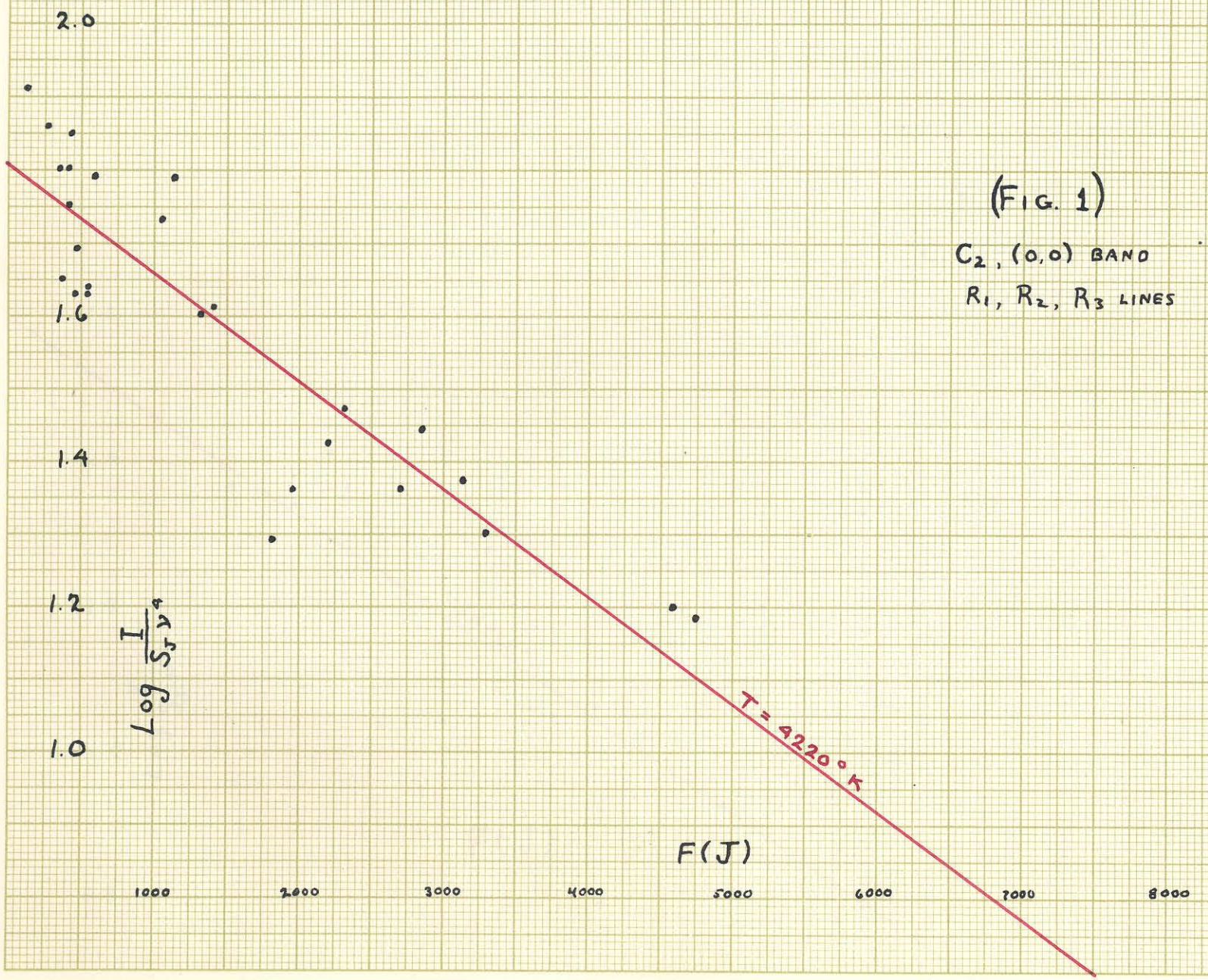

(FIG. 1)

C_2, (0,0) BAND

R_1, R_2, R_3 LINES

(FIG. 2)

C_2, (0,0) BAND

R_{23} LINES

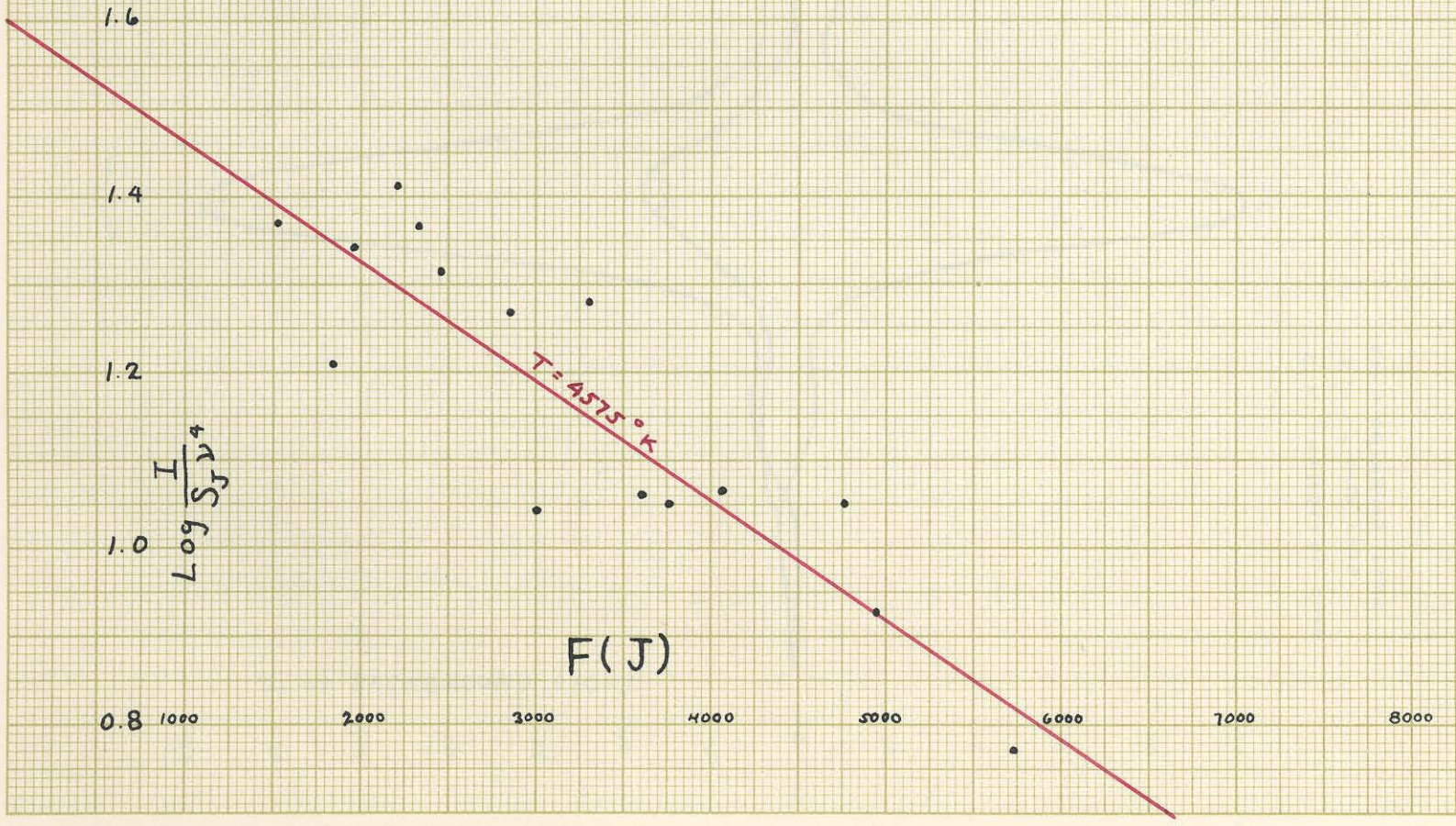

56

(FIG. 3)

λ 5525.556 Fe

CH = OBSERVED LINE
L = LIMB LINE
C = CORRECTED LINE

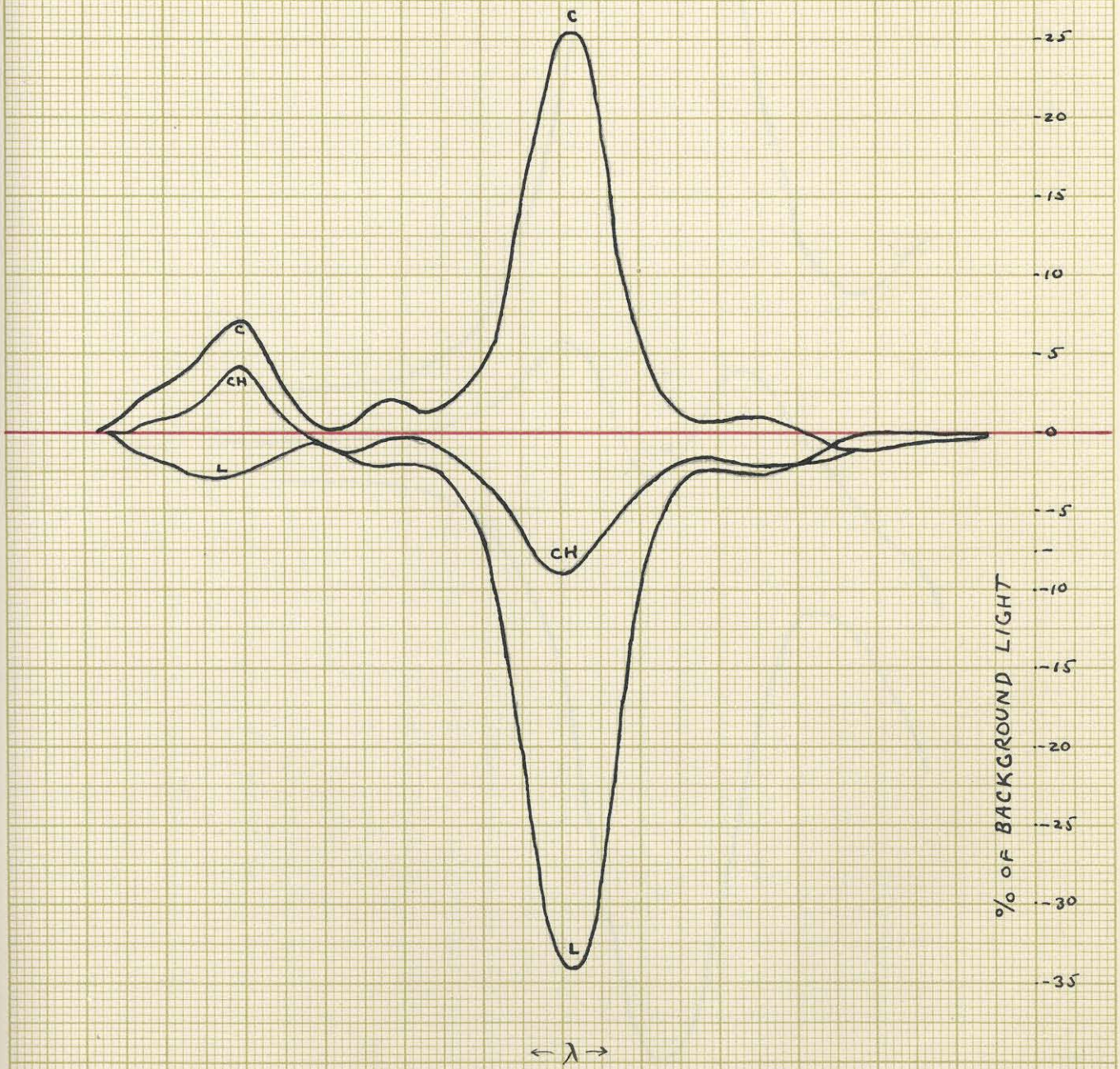

(FIG. 4)

λ5226.547 Ti II

CH = OBSERVED LINE

L = LIMB LINE

C = CORRECTED LINE

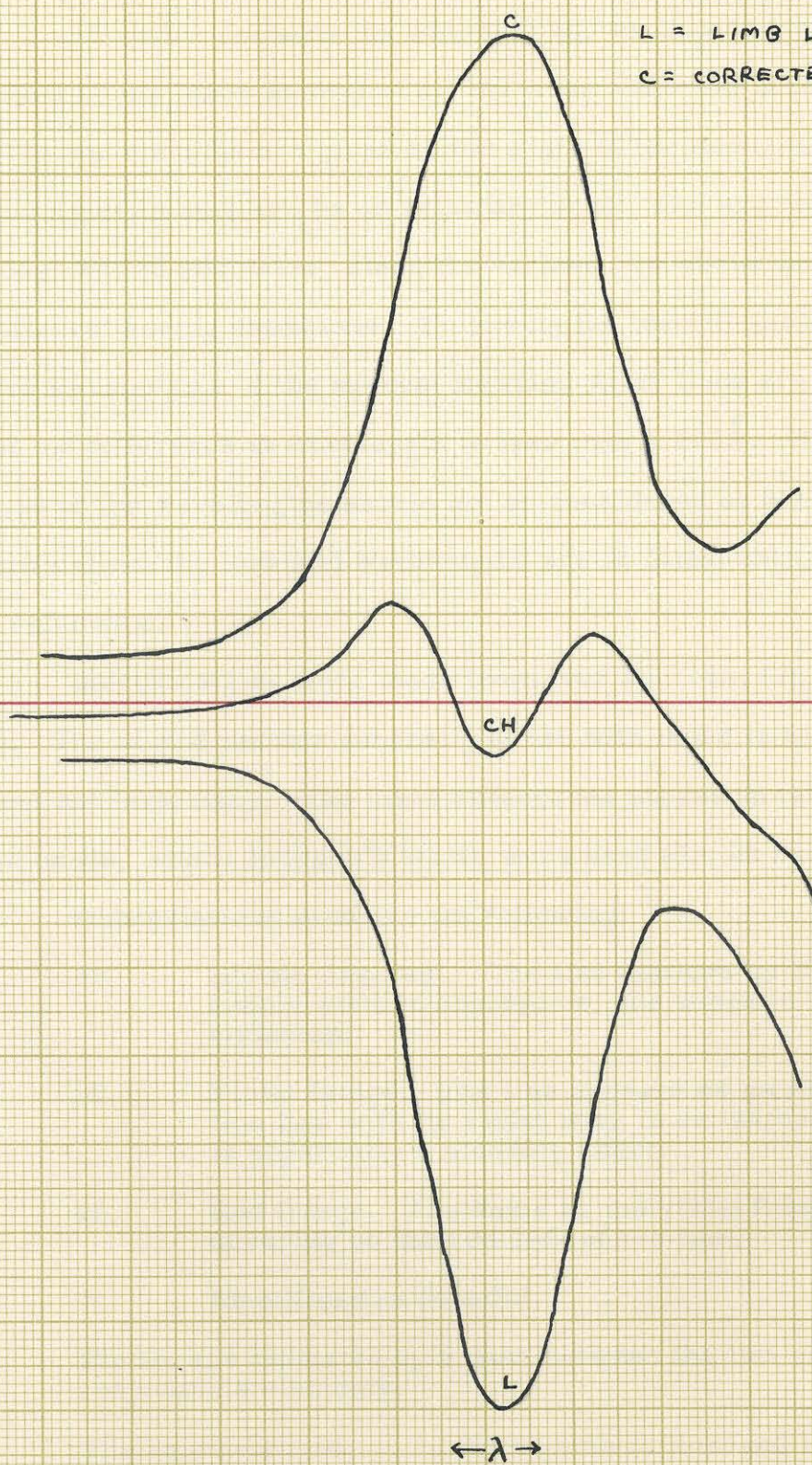

30
25
20
15
10
5
0
-5
-10
-15
-20
-25
-30
-35
-40

X. Appendix Table of Wavelengths of Observed Spectrum Lines in the Solar Chromosphere.

The table contains the wavelengths, estimated intensities, and identifications (when known) of all the lines observed in the present work. The wavelengths are given on the scale of the Rowland Atlas (2). The intensity estimates are on an arbitrary scale, and are not consistent throughout the spectrum, since the various exposures were made under different seeing conditions. Following the identifications of the lines, the wavelengths of the nearest Rowland Atlas lines are given, provided the difference in wavelength is less than 0.100Å. This separation of the wavelengths should not be considered as a criterion for identification; the Rowland wavelengths are included only for convenient reference.

Identifications were made from four sources; (2), (3), (14), and (15). The identifications generally agree with those in the Rowland Atlas, but not invariably. The main differences appear in faint lines of the Swan bands, where Johnson's tables were used almost exclusively.

Abbreviations used are the following:

dr	Double reversal. The line appears as if the center were in absorption, the wings in emission.
vf	Violet fringe. The line appears as an absorption line with its violet wing in emission. This is apparently a blending effect.
rf	Red fringe. The same as the violet fringe, but occuring on the red side of the line.
?	Identification doubtful.

Blends are indicated by a dash between the two or more responsible elements.

The abbreviations in the column of Rowland intensities

are those from the Rowland Atlas; e. g.

N nebulous

d double

Two lines deserve special mention. The λ5875Å HeI line is bisected by a low -sun atmospheric line, in the spectra. The two wavelengths given are for the two "components" thus formed. The λ6563Å H line is more than 1 Å wide on the plates. Therefore its wavelength could not be determined with any precision. This line was by far the most intense line on any of the spectrograms, and was consistently heavily overexposed.

Observed	Intensity	Element	Rowland	Rowland Intensity
5007.389	-1			
5008.562	-1			
dr.			.650	-2
5008.746	-1			
5009.434	-1	C_2	.429	-2
5009.559	-1			
dr.		Ti I	.654	-1
5009.743	-1			
5011.754	1	Ce ?		
5011.974	-1			
vf.		Fe	.077	4
5012.271	-1			
5013.789	-1	C_2	.778	-3
5016.606	-1	Sm II ?	.689	-3
5017.019	-1		.053	-3
5017.835	-2	C_2	.822	-2
5018.346	2			
dr.		Fe II	.452	4
5018.549	2			
5019.070	-2			
5019.381	-2			
5019.583	-2			
5019.823	-1			
rf.		Fe	.737	-1
5020.153	-1			
rf.		Ti	.033	2
5020.305	-2			
5020.581	-1		.500	-2
5020.724	-1	C_2	.698	-3
5021.794	0			
5022.985	0	Ti	.046	2
5023.987	-1		.015	-3

Observed	Intensity	Element	Rowland	Rowland Intensity
5025.794	0	C_2	.763	-2
5025.886	-1	C_2	.911	-2
5026.103	-1	Fe I		
5026.239	-1			
5027.548	-1	Fe I	.531	-3
5027.901	0		.925	-3
5028.250	-1			
rf		Fe I	.135	2
5028.379	-2		.361	-2
5028.504	-1		.543	-3
5028.788	-2			
5028.929	-2			
5029.909	0	C_2	.920	-3
5030.042	-1	C_2	.042	-3
5030.873	0		.882	-3
5030.962	1			
		Sc II	.026	3
5031.081	1			
5031.363	0			
5032.028	-1			
5032.116	-1		.077	-3
5032.873	0			
5032.977	0			
5033.525	-1		.539	-2
5033.669	-1	C_2	.660	-2
5033.779	-1	C_2	.785	-2
5034.198	-1		.179	-2
5034.419	-1	Pr II ?		
5035.648	1		.672	-2d ?
5036.091	-1		.158	-3

Observed	Intensity	Element	Rowland	Rowland Intensity
5037.050	-1			
5037.201	-1		.201	-3
5037.675	-1	C_2	.711	-2
5037.793	-1	C_2	.809	-2
5041.514	0		.459	-1
5041.973	1			
rf		Fe	.859	-1
5043.350	-1		.300	-2
5044.030	1	Ce II	.037	-2
5045.162	-1			
5045.260	0	C_2	.280	-1
5045.351	-1			
dr.		Ti I	.406	1
5045.505	-1			
5046.919	0		.931	-2
5047.057	-1		.125	-2
5047.258	0		.307	-2d
5047.385	0			
5047.557	0		.550	-3
5047.829	0			
5048.325	0			
dr.		Fe I	.441	3
5048.551	1			
5048.663	0			
5049.409	-1		.430	-3
5050.245	-1			
5050.712	-1		.742	-2
5050.878	-1	Gd II ?		
5051.771	1			
5051.997	0	Cr I ?	.906	0

Observed	Intensity	Element	Rowland	Rowland Intensity
5052.465	-1			
5052.635	0	C_2	.626	-1
5052.755	0	C_2	.740	-3
5052.881	1	Ti	.882	0
5054.076	-2	Ti I	.085	-2
5055.710	-2		.797	-3
5056.116	1	C_2	.129	-2
5056.265	1	C_2	.250	-2
5057.699	-1		.697	-3
5057.917 dr 5058.069	0 0	Fe I	.987	1
5058.305	-1		.243 ?	-2 N
5058.377	-1			
5058.571	-1	Fe I ?		
5058.806	-1	C_2	.811	-3
5058.911	-1	C_2	.932	-3
5059.429	-1		.397	-3
5059.781	-1	C_2	.786	-1
5059.928	0	C_2	.933	-3
5061.726	-1	C_2	.704	-1
5062.109	2	Ti I	.106	0
5062.360	-2		.352	-3
5063.168	1	C_2	.177	-1
5063.313	1	C_2	.301	-2
5063.740	1	Nd	.750	-3
5064.066	1	Ti I	.068	-1

Observed	Intensity	Element	Rowland	Rowland Intensity
5064.403	0		.380	-3N
5064.792	0		.812	-3
5065.764	-2	Ce ?	.713	-3
5066.731	1	C_2	.732	-1
5066.871	1	C_2	.863	-2
5068.202	0	C_2		
5069.357	1	Ti I	.417	-2d
5069.795	0	C_2	.796	-3
5070.016	0	C_2	.991	-1
5070.298	0	C_2	.297	-3
5071.769	0	C_2	.795	-2N
5071.891	-1	C_2	.858	-3
5072.366	-2	Ti II	.305	0
5073.456	1	C_2	.464	-1
5073.607	1	C_2	.603	-3
5073.883	-1			
5073.982	-1			
5075.356	2	C_2-CeII	.306	-1
5075.798	-1	Sc	.815	-3
5075.908	-1			
5076.602	0	C_2	.633	-1
5076.762	0	C_2	.776	-2
5077.013	-1			
5077.169	-1	Nd ?		
5077.386	-1	C_2	.388	-2
5077.508	-1			

Observed	Intensity	Element	Rowland	Rowland Intensity
5077.852	0		.838	-3d
5078.210	-1	C_2		
5078.361	1	C_2	.366	-2
5080.107	1	C_2	.113	-3
5080.871	-1		.937	-3
5081.025	-1			
5081.585	2	Sc I	.590	-2
5081.772	1	C_2	.768	-2
5082.471	0	C_2		
5082.865	0		.899	-3
5083.061	1	C_2	.033	-2d
5083.731	1	Sc I	.706	-2
5084.705	0	C_2	.705	-2
5084.827	0	C_2	.846	-2
5085.564	1	Sc I	.497	0
5085.759	-1			
5085.824	0			
5086.017	-1			
5086.252	1	C_2	.251	-1
5086.420	1	C_2	.399	-2
5086.801	-2	C_2	.776	-2
5086.947	1	Sc I	.933	-3
5087.387	1	Y II	.428	1
5087.477	1			
5087.862	-2	Co	.848	-3N
5088.018	-1	C_2	.004	-2

Observed	Intensity	Element	Rowland	Rowland Intensity
5089.078	0	Eu ?		
5089.215	0	C_2	.217	-2d
5089.377	0	C_2	.371	-3
5089.852	1	Nd II	.834	-3
5090.352	0	Dy ?	.399	-3
5090.572	-1	La II ?		
5091.169	0	C_2	.183	-3
5092.800	2	Nd II	.807	-2
5093.722	-2	C_2	.688	-3N
5094.035	1	C_2	.029	-2N
5094.138	0	C_2	.148	
5094.279	1			
vf		Ni	.420	0
5095.164	-1	C_2	.178	-1d ?
5095.328	-1	C_2	.342	-1
5095.468	-2	C_2	.509	-3
5095.982	-1	Gd ?		
5096.052	0		.045	-3
5096.520	-1	C_2 ?	.490	-3
5096.761	0	Sc I	.738	-2
5097.723	0	C_2	.714	-3
5098.169	1	C_2	.132	-1 N
5098.335	1	C_2	.322	-2 N
5099.789	-1	C_2	.788	-2
5100.665	1	Fe II	.658	-1
5100.865	0	C_2	.859	-2
5100.944	0	C_2	.939	-2

Observed	Intensity	Element	Rowland	Rowland Intensity
5101.093	1	Sc I	.082	-2
5101.492	-1	Fe II	.486	-2
5101.641	-1		.621	-3
5102.399	2	C_2^-	.430	-2
5102.550		C_2		
5103.106	1	C_2	.128	-3
5103.755	1	C_2	.741	-2
5103.933		C_2	.915	
5105.000	-2			
5105.232	1		.188	-3
5105.365	1	C_2	.368	-2
5106.375	0	C_2	.388	-3
5106.612	1	C_2	.605	-2
5107.862	0			
5107.398	0	C_2	.889	-2
5108.226	-2	C_2	.192	-2
5108.330 dr.	0	Co I ?	.396	-1
5108.490	0			
5108.551	0			
5108.710	0			
5108.910	0	Co I	.916	-3
5109.143	1	C_2	.124	-2d
5109.313	0	C_2	.308	-3
5109.505	0	C_2		
5110.028	0	C_2	.021	-3
5110.180	0	Zr I ?		

Observed	Intensity	Element	Rowland	Rowland Intensity
5110.561	-1	Sm ?		
5110.674	0	C_2		
5110.810	0	C_2		
5111.624	0	C_2	.635	-2
5111.739	0	C_2	.745	-3
5111.866	0	C_2	.882	-2
5112.288	4	Zr II	.291	-2
5112.961	-2		.986	-2
5113.088	1	Cr I	.131	-1
5144.244	1	C_2	.264	-2d
5114.333	0	Eu ?		
5114.546	2	La II-C_2	.516	-2d
5114.630	2			
5115.540	-1	C_2		
5115.679	-1	.	.676	-3
5115.888	1	C_2	.878	-3
5116.650	1	C_2	.682	-3
5116.770	1	C_2	.777	-2
5116.911	1	C_2	.904	-2
5117.180	1	Ce II	.167	-3
5118.075	0	C_2	.074	-3
5118.184	0	C_2	.185	-3
5118.769	-1		.820	-2d
5119.123	1	Y II	.125	-1
5119.238	1	C_2	.201	-3
5119.389	1	C_2	.388	-2

Observed	Intensity	Element	Rowland	Rowland Intensity
5119.637	0		.653	-2
5119.764	-1		.775	-3
5120.338	1	C_2	.349	-2
5120.458	1	Ti	.425	0
5120.635	1	C_2	.635	-2
5120.739	1	C_2	.726	-3
5121.010	-1	C_2	.029	-3
5121.145	-2			
5121.344	0	C_2		
5121.452	1	C_2	.441	-3
5122.311	-1	C_2	.313	-3
5122.462	-1	C_2	.445	-3
5122.794	0	CoI-C_2	.800	-2
5123.007	3	La II	.010	-2
5123.218	1	Y II	.222	0
5124.052	0	C_2	.051	-2
5124.192	-1	C_2	.196	-3
5124.767	-2	C_2	.771	-3
5124.951	-1	Zr II		
5125.332	0	C_2		
5125.497	0	C_2	.477	-3
5125.715	1	Co I		
5125.974	1	C_2	.999	-3
5126.612	1	C_2		
5126.716	-1	C_2	.688	-2
5128.184	1	C_2	.215	-3

Observed	Intensity	Element	Rowland	Rowland Intensity
5128.321	1	C_2	.319	-3
5128.506	1	C_2	.493	-2
5128.740	-1	C_2		
5128.875	-2	C_2	.913	-2
5128.975	-2	C_2		
5129.246	0	C_2		
5129.708	1	C_2		
5130.276	1	C_2		
5130.444	0	C_2		
5130.597	4	Nd II-C_2	.590	-2
5131.590	0	C_2	.604	-3
5131.687	0	C_2		
5132.346	2	Nd II-C_2	.356	-3
5132.500	0	C_2	.506	-2
5132.682	2	Fe II	.676	-1
5133.472	1	Co I	.487	-2
5133.829	0	C_2	.821	-3N
5134.315	0	C_2	.338	-3
5134.485	-1	C_2	.530	-2
5134.684	0	C_2	.682	-2
5135.136	0	Pr II	.106	-3
5135.579	1	C_2	.585	-2
5135.712	0	C_2	.713	-2
5136.279	-1	C_2	.276	-2
5136.445	1	C_2	.458	-3
5136.653	0	C_2	.668	-3
5136.814	1	Fe II	.802	-2

Observed	Intensity	Element	Rowland	Rowland Intensity
5137.584	1	C_2	.586	-2
5137.705	1	C_2	.697	-2
5138.115	0	C_2	.112	-3
5138.315	0	C_2	.351	-3
5138.520	0	C_2	.523	-3
5139.655	0	Cr I	.650	-1
5139.940	0	C_2	.927	-3
5140.145	0	C_2	.169	-3
5140.380	0	C_2	.386	-3
5141.197	1	C_2	.219	-2
5141.328	1	C_2	.330	-3
5142.121	0	C_2	.112	-3
5142.360	0			
5143.345	0	C_2	.344	-2
5143.605	0	C_2	.597	-2
5143.859	0	C_2	.864	-3
5144.567	1	C_2	.591	-2
5144.927	-1	C_2	.931	-3
5145.223	0	C_2	.236	-3
5145.477	-2	Ti I	.470	0
5145.589	-2			
5146.108	2	Fe II-C_2	.124	-1
5146.228	-1			
5146.766	1	Co I	.778	-2d ?
5147.576	1			
5147.697	1	C_2	.704	-2
5147.823	1	C_2	.825	-2

Observed	Intensity	Element	Rowland	Rowland Intensity
5149.085	1	Na -C_2	.100	-2
5149.221	0	C_2	.225	-2
5149.341	-1	C_2	.345	-3
5150.557	1	C_2	.569	-2
5150.678	1	C_2	.675	-3
5151.038	-1			
5151.177	-1	C_2	.177	-3 N
5151.328	-1			
5151.523	0	C_2		
5152.519	-1	C_2	.533	-3
5153.149	1	C_2	.170	-3
5153.779	1	C_2	.818	-3d
5154.008	0	Ti II	.077	2
5154.317	1	C_2	.338	-3
5154.438	1	Fe II	.412	-2
5155.004	-1	C_2		
5155.519	1	C_2	.527	-2
5155.656	1	C_2		
5155.925	0			
5156.350	0	Co I	.363	-2
5156.556	1	C_2	.561	-3
5156.679	1	C_2	.656	-1 N
5156.740	1	C_2		
5157.433	0	La II		
5157.622	1	C_2	.616	-2
5157.767	0	C_2	.748	-2
5157.899	-1	Sm ?		

Observed	Intensity	Element	Rowland	Rowland Intensity
5158.517	1	C_2	.534	-2
5158.684	1	C_2	.665	-3
5158.850	0	Co I	.859	-3 N
5159.466	1	C_2	.467	-2
5159.618	0	C_2	.609	-3
5159.775	-2		.779	-3
5160.199	0	C_2		
5160.249	1	C_2	.251	-1 N
5160.398	1	C_2	.386	-3
5160.570	-2	Sm ?		
5160.723	-2			
5161.049	1	C_2	.026	-2
5161.196	1	C_2	.185	-2
5161.700	1	C_2	.681	-3
5161.858	0	C_2		
5161.988	-1		.985	-3
5162.395	0	C_2		
5162.522	0	C_2	.522	-3
5162.608	-2			
5162.874	0	Sm ?		
5162.926	0	C_2	.906	-2
5163.069	0	C_2	.032	-2
5163.175	-2	C_2	.159	-3
5163.428	1	C_2	.417	-2
5163.532	1	C_2		
5163.605	1	C_2	.588	-2

Observed	Intensity	Element	Rowland	Rowland Intensity
5163.819	0	Pd ?	.839	-3
5163.866	-1	C_2		
5164.032	-1	C_2	.004	-3
5164.198	0	C_2	.236	-2
5164.265	0	C_2		
5164.393	0	C_2	.394	-3
5164.492 dr	-1	Fe I	.554	1
5164.651	-1			
5164.784	0	C_2	.782	-3
5165.020	0	C_2	.041	-3
5165.130	0	C_2	.129	-3
5165.256	1	C_2	.248	-3
5166.087	-1	Nd		
5167.211	2	Mg I	.330	15
5167.431	1			
5167.607 rf	2	Fe	.510	5
5167.891	-2		.956	-3
5167.928	0	Nd	.956	-3
5168.794 dr	1	Fe I	.910	3
5168.975 bl dr	2	Fe II	.052	4
5169.150	5			
5169.390	-1		.302	-1
5170.516	-2	Ti	.488	-3
5170.648	-2		.600	-2
5170.874	-2			
5170.959	-2			

Observed	Intensity	Element	Rowland	Rowland Intensity
5171.036	-2			
5171.514 vf	1	Fe	.612	6
5172.560 dr	3	Mg I	.700	20
5172.835	3			
5173.917	2	Pr II ?	.911	-3
5175.864	-1			
5176.301	1	Gd II ?		
5176.440	0	Eu ?		
5176.690	-1			
5176.807	0	V I	.788	-2
5177.542	0			
5178.194	0			
5178.937	0	Fe II		
5179.028	0			
5182.588	0	Nd	.596	-3
5183.327	-1			
5183.457 dr	2	Mg I	.621	30
5183.754	2			
5187.459	2	Ce II	.456	-2
5188.230	-1	La II	.245	-3
5188.620 dr	1	Ti II	.700	2
5188.765	1			
5189.585	0	Ti I	.580	-2
5191.606	3	Zr II	.604	-2
5192.005	-2	Cr I	.992	-1

Observed	Intensity	Element	Rowland	Rowland Intensity
5192.622	2	Nd II	.622	-2
5193.833	-2		.864	-3
5194.201	-2			
5194.459	-2			
5194.756	-1	Ce ?		
5195.316	-1	Pr II		
5196.344	-1	Cr I	.449	0
5197.527 dr	2	Fe II	.578	2
5197.625	2			
5199.804	-2			
5199.936	-2			
5200.133	0	Cr I	.190	-1
5200.376 dr	1	Y II	.417	0
5200.457	1			
5201.092	-2	Ti I	.095	-2
5201.776	-2			
5203.506	-2		.493	-2
5204.143	-1	La II		
5205.512	-1	Ce ?		
5205.681 dr	1	Y II	.732	0
5205.780	1			
5205.949 dr	0	Cr I	.046	5
5206.145	0			
5206.296	-1			
5206.561	0	Pr II	.547	-2
5207.868	0	Ti I	.874	-3

Observed	Intensity	Element	Rowland	Rowland Intensity
5208.033	0	Cr I		
5208.197	-1			
5209.048	-2			
5210.052	0	Co I	.041	-3
5210.842	-1	Co I	.852	-2
5211.727	-1	Sm ?		
5211.851	-1	La I		
5212.271	1	Cr I		
5212.383	1	Nd II	.341	-3
5212.668	0	Co I	.697	-2d ?
5212.732	0			
5212.994	-1	Ti I	.993	-3
5214.136	0	Cr I	.125	-1
5215.666	0	Nd		
5216.589	-1	V I		
5216.731	-2	Pr ?		
5217.168	-2			
5218.337	-1			
5218.430	-1	Sm ?		
5219.043	1	Co I	.028	-3
5220.116	1	Pr II	.092	-2
5220.896	-1	Cr I	.920	-2
5221.569	-1	Nd		
5222.511	0	Co I		
5222.678	0	Ti I	.691	-1
5223.625	0	Ti I	.632	-2

Observed	Intensity	Element	Rowland	Rowland Intensity
5224.550	0	Cr I	.552	-1
5226.472	1			
dr		Ti II	.547	2
5226.610	1			
5227.082	0			
dr		Fe I	.194	5d ?
5227.301	0			
5228.594	-2	Y I ?	.563	-3
5230.403	-1	Co I ?	.389	-3
5230.980	-1	Ti I	.987	-3
5232.513	-1	Cr II	.517	-2
5232.853	0			
dr		Fe I	.954	7
5233.038	0			
5234.046	-1	V I	.092	-3
5234.206	1	Nd II	.217	-2
5234.569	2			
dr		Fe II	.632	2
5234.684	2			
5235.618	-1			
5237.080	1	Co ?	.091	-3
5237.282	-1			
dr		Cr II	.327	1
5237.376	-2			
5238.524	-1	Ti I	.570	-2 N
5238.671	-2			
5239.084	-1			
5239.771	1			
		Sc II	.825	1
5239.869	1			
5240.474	-1	Cr I	.476	-2
5240.875	0	V I	.877	-2
5241.338	-2			

Observed	Intensity	Element	Rowland	Rowland Intensity
5241.795	-1			
5243.359	0	Cr I	.363	-1
5243.520	-2	Cr II ?	.472	-3
5245.821	-2			
5245.930	-2	Ce ?		
5246.127	-2	Ti I	.147	-3
5246.649	-1			
5247.298	-1	Ti I	.299	-2
5249.429	0	Cr II ?		
5249.586	3	Nd II	.587	-3
5250.013	0	Co I	.029	-3
5250.822	2	Nd II		
5252.668	0			
5252.807	-1			
5254.655	0	Co I	.665	-3
5254.884 vf ?	0	Cr-Fe ?	.955	3
5255.524	3	Nd II	.522	-3
5255.824	0	Ti I	.805	-3
5256.937	1	Fe II	.934	-1
5257.606	0	Co I	.648	0
5258.473	-2			
5258.704	-2			
5259.742	2	Fe	.746	-3
5259.979	-1	Ti I	.979	-2
5260.288 dr ?	-1	Ca I ?	.395	0
5260.499	-1			
5262.256	-1	Ca I	.252	3

Observed	Intensity	Element	Rowland	Rowland Intensity
5263.077	-2	Fe ?	.072	-3
5263.739	-1	Cr I	.723	-2
5264.810	2	Fe II	.810	0
5265.169	-1	Cr I	.154	-1
5264.334	0			
5265.848	0			
vf ?		Ti I ?	.966	0
5266.079	-1	V I ?	.079	-2 N
5266.307	1	Co I	.315	-2
5447.982	0	Ti I	.938	-3
5448.255	0			
5449.270	1	Nd ?		
5450.407	-1			
5450.604	-1			
5451.143	1	Nd II	.126	-2
5451.877	-1			
5452.020	-1	Ti I	.957	-3
5452.295	0	Co I	.301	-2
5453.099	0		.090	-3
5454.120	1		.123	-2
5454.586	3	Co I	.580	-1
5456.127	-1	Si II	.116	-3 N
5456.297	-1			
5456.636	-1			
5457.118	0		.108	-2
5457.332	0			
5457.593	0	Zr I ?		

Observed	Intensity	Element	Rowland	Rowland Intensity
5457.688	0			
5458.420	0			
5458.676	0	La II		
5459.168	0			
5460.737	0	Zr I ?	.701	-3d ?
5462.251	-1		.276	-3
5463.861	0		.835	-3
5464.197	1			
dr		Fe I	.290	0
5464.431	1			
5467.388	-1		.403	-2
5467.561	-1		.571	-3
5468.179	-1	Ni I ?	.118	-1
5468.381	3	Ce II - Sc I	.399	-2d ?
5470.443	1	Co I	.448	-2
5472.304	3	Ce II	.302	-2
5473.384	2	Y II	.393	-2
5473.610	-1	Ti I	.557	-2 N
5474.122	1	Fe I ?	.098	-3
5474.467	1	Ti I	.467	-2
5474.756	0	Nd II	.761	-3N
5475.724	0		.737	-3N
5477.530	0		.506	-2Nd
5477.755	0	Ti I	.707	-1
5478.028	-1			
5478.250	0			
5478.365	1	Cr II	.377	-1
5480.741	1	Y II	.763	-2

Observed	Intensity	Element	Rowland	Rowland Intensity
5481.731	0	Pr ?	.740	-3
5482.304	0	La II	.268	-2N
5482.577	0		.606	-2N
5482.984	0		.930	-3
5483.240	0			
rf ?		Fe I ?	.110	1
5483.920	0	Co I	.911	-2
5484.053	0		.043	-2
5484.630	1	Sc I	.645	-2
5484.886	-2		.822	-3
5485.556	0		.556	-2
5485.722	2	Nd II	.714	-3
5486.128	0	Sr I	.119	-2
5487.325	0		.333	-3N
5487.637	1			
dr		Fe I	.757	3
5487.907	1			
5488.220	0	Ti I		
5488.389	-1		.346	-3
5489.686	1	Co I ?	.691	-2
5490.044	-1			
dr		Ti I	.161	0
5490.297	0			
5490.716	2	Ti II ?	.703	0
5491.691	1	Pr ?	.695	-3
5492.209	-1		.222	-2
5492.364	-1	Pr ?	.364	-2
5492.903	1		.893	-1
5493.379	1	Nd ?	.356	-3

Observed	Intensity	Element	Rowland	Rowland Intensity
5493.634	0		.662	-3
5494.041	0	Nd ?		
5494.330	0		.333	-3
5494.877	-1	Ni I	.893	-1
5495.238	-1			
5495.652	1	Co I	.713	-2
5497.165	0		.122	-2
5497.419	2	Y II	.421	-3
5497.657	1	Fe II		
5497.904	0	Ti I	.902	-2
5498.523	-1			
5498.717	0	C_2	.751	-3
5499.015	0	C_2	.030	-2
5499.178	0	C_2	.172	-3
5499.779	-1		.772	-3
5500.079	-1			
5500.599	-1	C_2	.607	-3
5500.972	-1	C_2	.989	-2
5501.605 vf	1	Fe	.479	5
5501.922	-1			
5502.105	0	Cr II	.093	-1
5502.579	-2		.579	-3
5502.940	0		.949	-1
5503.256	1	C_2-Co I	.239	-1
5503.920	2	Ti I	.906	0
5504.250	0	Mn I	.226	-3

Observed	Intensity	Element	Rowland	Rowland Intensity
5504.463	0		.394	-1
5504.679	0	C_2	.662	-3
5506.022	0	C_2	.038	-3
5506.173	0	C_2	.190	-2
5506.328	-1	C_2	.371	-2
5506.513	0	Mo I	.514	-2
5507.756	0	V I	.780	-2
5508.420	-1		.420	0
5508.647	-1	Cr II	.635	0
5509.113	-2	Nd ?	.115	-3
5509.916	4	Y II -Cr I	.914	0
5510.638	0	C_2	.623	-1
5510.784	0	Cr II	.736	-1
5511.458	0	C_2	.438	-2
5511.661	-1	Fe	.666	-3
5512.074	4	Ce II	.060	-1
5512.352 rf	-1	Fe I	.267	1
5512.563	-2	Ti I	.537	2
5513.602	0	Y I ?	.563	-3
5514.206	0	Sc I	.224	-3
5514.379	1	Ti I	.355	2
5514.576	2	Ti I	.546	2
5515.354	-1	C_2	.358	-2
5516.027	-1	Sm ?	.046	-3 N
5516.584	0	C_2	.501	-2
5516.930	-1			

Observed	Intensity	Element	Rowland	Rowland Intensity
5517.175	-1			
5517.337	-1	La I ?	.382	-3
5518.052	0	Zr I ?	.099	-2
5518.198	0	C_2	.170	-3
5518.505	0	Ce II	.546	-3
5518.670	-1	Nd		
5519.393	1	-C_2?	.425	-2
5519.575	1	Fe I	.589	0
5519.860	0	C_2	.860	-2N
5520.013	0	Nd ?	.038	-3
5520.502	2	Sc I	.519	-1N
5521.274	-1	Fe I	.303	-1
5521.583	2	Y II - Y I	.591	-1
5521.844	-1	Sr I ?	.793	-3N
5522.169	-1	Mn - Nd ?	.198	-3N
5522.333 dr	-1	Fe I	.456	2
5522.578	-1			
5523.192	0		.260	-2
5523.583	0	Ti I	.574	-2N
5524.085	0	Co I	.000	-1
5524.481	0	C_2	.475	-2
5524.588	0	C_2	.576	-3
5524.766	-1		.801	-2
5524.967	0	Co I	.011	-2
5525.151	1	Fe II	.138	-1
5525.418	0	Fe I ?		

Observed	Intensity	Element	Rowland	Rowland Intensity
5526.167	-1	C_2	.195	-2N
5526.801	1	Sc II	.823	3
5526.879	2	Ce II		
5527.552	-2	Y I - Ti I	.586	-2d
5527.875	0	C_2	.874	-3N
5528.089	0		.087	-2
5529.056	0	Nd ?		
5529.341	0		.354	-2
5530.011	0			
5530.457	0	Ti I - Nd ?	.493	-1 N
5530.923	0			
5531.330	-1			
5531.875	1			
5532.137	1	C_2	.142	-2
5532.365	1	C_2	.360	-2N
5533.064	0	Mo I	.037	-2
5533.442	0	C_2	.443	-2
5533.840	1	Nd ?	.800	-2d
5534.552	-2			
5534.858	5	Fe II	.849	2
5535.178	0	C_2	.187	-2N
5535.731	0		.773	-3
5535.881	-1		.860	-3
5536.082	0	C_2	.088	-2
5536.304	1	C_2	.280	-2
5536.448	0	Mn	.467	-3
5536.687	0	Zr ?		

Observed	Intensity	Element	Rowland	Rowland Intensity
5536.866	-1	Eu ?	.819	-3
5537.616	-1			
5537.893	0			
5538.294	-1		.314	-3
5539.058	-1	C_2	.061	-3
5539.972	-1	C_2	.980	-3
5540.183	-1	C_2	.181	-2N
5540.467	-1	C_2	.449	-2N
5540.706	-1	C_2	.728	-2
5540.905	-1		.897	-2
5541.749	-1			
5541.919	-1			
5542.768	-1	Sm ?	.756	-3
5542.947	-1		.899	-3
5543.357	-1	Sr I ?	.413	-3
5544.193	0		.173	-2
5544.344	-1		.347	-3
5544.627	3	Y II	.618	-2
5545.988	2	Y II	.934	-2
5547.683	-1	Nd ?	.697	-3N
5548.185	1	Gd ?	.199	-3
5548.335	1		.321	-3
5548.468	1	Nd II	.483	-3
5548.718	0	Nd		
5549.525	0	Fe I ?	.534	-3
5549.767	1			
5550.065	1	Ce ?		

Observed	Intensity	Element	Rowland	Rowland Intensity
5550.786	-1			
5551.546	1		.553	-2N
5551.761	1	Fe I	.781	-3N
5551.972	1	Mn I	.979	-2
5552.231	1	Sc II	.238	-2
5552.425	-1	Mn ?	.459	-3d ?
5552.823	0	Nd ?	.854	-3
5553.108	1		.132	-2N
5553.306	-1			
5554.237	0	Cr ?	.245	-3N
5554.469	-1			
5554.647	-1		.665	-3
5555.113	0			
5555.230	0	Fe I ?	.180	-3
5555.355	0		.357	-3
5555.470	0		.468	-3
5555.645	0		.645	-2
5555.834	0			
5556.733	0	Mo ?	.718	-3N
5556.950	1	Ce II	.918	-2
5557.476	2	V I ?	.495	-2
5557.796	0		.731	-2N
5558.116	0		.176	-3
5558.830	2	Co I	.853	-2d ?
5559.064	1		.066	-2d ?
5559.282	0			
5559.732	1	Gd ?		

Observed	Intensity	Element	Rowland	Rowland Intensity
5559.864	1		.891	
5560.374			.432	-3
5560.679	1	Gd II	.696	-3
5561.451	-1	Pr ?	.484	-3N
5561.713	-1			
5562.231 dr?	1		.285	-3
5562.333	1			
5562.526	1	Mo ?	.502	-3
5562.848	0	Sm ?		
5563.805	1			
5563.954	-2			
5564.600	-1	C_2		
5564.942	-1	C_2	.975	-3
5565.310	-1			
5565.490	2	Ti I	.487	-1
5565.944	0	C_2	.956	-3N
5566.703	-1		.731	-2
5567.141	-1		.151	-3N
5567.464	0	Fe I	.402	2
5568.567	-1			
5569.039	0		.033	-3
5569.886	0	C_2		
5570.441	0	Mo I ?	.399	-2
5570.595	0	Mo I ?	.611	-2
5570.761	-2	C_2	.766	-3
5572.127	0	C_2	.154	-2N

Observed	Intensity	Element	Rowland	Rowland Intensity
5572.302	-1		.356	-3
5572.415	-1	C_2	.453	-3
5573.583	0	C_2	.545	-3
5573.755	-1	CoI	.757	-2
5573.996	-2			
5574.876	-1		.911	-2
5575.099	-1	C_2	.093	-3
5575.510	-1	C_2	.549	-3
5575.642	-1	C_2	.680	-3
5575.799	-1	C_2	.862	-3
5576.211	1	C_2		
5576.399	0		.372	-3
5576.874	0			
5577.359	1	[illegible]	.344	-2
5577.570	0	C_2	.566	-3
5578.516	0	C_2	.522	-3
5579.034	-1	C_2	.043	-3
5579.163	0	Ti I	.164	-3
5579.464	0	C_2	.494	-3
5579.696	0			
5580.438	0	C_2	.456	-2
5580.664	0		.663	-3
5581.499	-1		.524	-3
5581.730	-1	C_2	.706	-3N
5585.092	0	C_2	.044	-3
5586.011	0	V I	.006	-3
5586.309	0		.281	-2

Observed	Intensity	Element	Rowland	Rowland Intensity
5586.718	0	Fe I		
5586.913	0			
5587.069	0			
5587.253	0			
5587.724	1		.731	-3
5589.710	0	Ti I		
5590.501	-1	C_2	.509	-3
5590.711	-1	Co I - C_2	.711	-2
5590.841	-1		.823	-2
5591.371	-1	Sc I	.370	-2
5591.720	-1			
5592.156	1	Ni I	.155	0
5592.403	0	V I	.428	-2
5592.717	-1		.666	-2
5593.028	-2	C_2		
5593.251	-1	C_2	.243	-3
5593.398	-1	C_2	.465	-2
5593.637	0			
5595.698	-1	C_2	.691	-3
5596.153	0	C_2	.187	-2
5597.913	-1	Ti I		
5598.324	0	Fe I	.307	1
5598.634	0	C_2		
5598.838	0		.819	-2
5599.050	-1		.955	-3
5599.848	-1			

Observed	Intensity	Element	Rowland	Rowland Intensity
5600.024	0	Ni I	.028	-1
5600.418	-1	.	.463	-3
5600.690	-1	C_2		
5600.882	-1	C_2		
5601.029	-2	Mo ?		
5601.176	-1	C_2		
5601.407	-1	Nd ?	.439	-3
5601.640	-2	Pd ?		
5602.652	-1	Nd ?		
5603.319	-2	C_2	.302	-3
5603.665	-1	Nd II		
5604.978	0	V I	.957	-2
5605.651	-1	C_2	.650	-2
5604.978	0	V I	.957	-2
5605.651	-1	C_2	.650	-2
5605.905	-1	C_2	.908	-2
5606.078	-2	C_2	.054	-3
5607.126	-1	Fe II ?	.158	-3
5607.570	-1	C_2	.547	-3
5607.827	-1	C_2	.845	-3
5608.166	0	C_2	.179	-2
5608.328	-1	C_2	.311	-2
5609.087	0			
5609.238	-1	Mo ?	.181	-3
5609.656	-2	C_2	.687	-3
5610.242	1	Ce II-C_2	.253	-2
5610.866	-1			

Observed	Intensity	Element	Rowland	Rowland Intensity
5611.212	-1	Nd?		
5611.469	-1			
5611.707	-1	C_2	.641	-2
5612.051	-1	C_2		
5612.335	1	C_2	.360	-2
5612.504	-1	C_2	.497	-2
5613.672	0	Ce II- C_2	.716	-2N
5614.031	-1	C_2	.040	-3N
5614.245	0	C_2	.284	-1N
5614.415	-1	C_2	.419	-3
5614.781	1	Ni I	.784	0
5615.939	-1	C_2		
5616.164	0	C_2	.191	-2
5616.361	-1	C_2	.328	-3
5616.864	-2			
5617.008	-2			
5617.235	0	Fe I	.238	1
5617.717	-1	C_2	.759	-3
5617.899	-1	C_2	.917	-2
5618.096	-1	C_2	.079	-3N
5618.856	-1	C_2	.847	-2N
5618.989	-1	Nd ?	.979	-3N
5619.480	-1	C_2	.424	-3
5619.765	-1	C_2	.824	-2
5619.905	-1	C_2		
5620.198	-1	Ti ?	.239	-3d
5620.638	1	Nd II	.649	-3

Observed	Intensity	Element	Rowland	Rowland Intensity
5621.194	0	C_2	.225	-2N
5621.404	-1	C_2	.382	-2N
5621.714	-2	C_2		
5621.990	-2			
5622.784	1	C_2	.783	-2
5623.036	0	C_2		
5624.188	0	C_2	.195	-3N
5624.890	1	V I	.883	-2
5625.081	-1		.091	-3d ?
5625.315	1	Ni I	.331	0
5625.567	0	C_2	.542	-2
5625.749	0	C_2	.691	-1
5625.975	-1	V I	.032	-2N
5626.114	-1			
5626.790	0	C_2	.821	-2
5626.983	0	C_2		
5627.499	1	Fe II	.510	-2
5627.650	-1	V I	.646	-1
5628.018	0	C_2	.026	-2N
5628.191	-1	C_2	.198	-3
5628.371	0	Ni I	.358	-1
5629.074	-1	C_2	.048	-2
5629.300	-2	C_2	.240	-3
5630.111	-1	C_2	.099	-2
5630.316	-1	C_2	.302	-3
5630.963	-1	C_2	.980	-3
5631.228	-1	C_2		

Observed	Intensity	Element	Rowland	Rowland Intensity
5631.829	0	C_2	.835	-2N
5632.073	0	C_2	.018	-2
5632.496	-1	V I	.458	-2d
5632.622	-1	C_2		
5632.778	-1	C_2	.757	-3
5633.165	0			
5633.278	0	C_2	.227	-2d ?
5633.443	0	C_2	.445	-3N
5633.754	1	C_2	.753	-3
5634.233	0	C_2	.232	-3d
5634.326	0	C_2		
5634.483	0	C_2	.526	-3
5634.682	0	C_2		
5634,867	1	C_2		
5635.196	0	C_2	.198	-3
5635.351	0	C_2	.345	-3
5635.517	0	C_2	.522	-3
5635.941	-1			
5636.100	-1	Co I	.125	-3
5636.418	-1		.474	-2N
5636.928	-1			-3d
5636.928	-1		.899	-3d
5637.122	0	Ni I	.126	1
5637.402	0	Fe	.417	1
5637.755	-1	Co I	.714	-2N
5638.019	-1			
5638.136	-1			

Observed	Intensity	Element	Rowland	Rowland Intensity
5640.987	1	Sc II	.992	1
5641.890	-1	Ni I	.898	0
5642.353	-1	Cr I	.391	-1
5643.080	0	Ni I	.088	0
5643.310	-1		.289	-3N
5644.142	2	Ti I	.149	0
5646.105	0	V I	.108	-2N
5647.229	0	Co I	.243	-1
5647.870	-2		.905	-3
5648.280	-2		.289	-2
5648.568	1	Ti I	.581	-1
5649.416	0	Cr I	.397	-1N
5649.718	0	Ni I	.684	0d
5649.973	-1	Fe I	.999	1
5650.165	-1		.206	-3
5650.686	-1	Fe I	.697	1
5650.905	-2		.885	-3
5654.787	-1		.778	-3N
5655.189	0	Fe I	.186	1
5655.382	-1		.345	-3
5655.487	-1	Fe I	.502	2
5657.467	0	V I	.454	-2
5657.661	-1		.677	-3
5657.908	2	Sc II	.883	2
5658.345	2	Sc II	.349	0

Observed	Intensity	Element	Rowland	Rowland Intensity
5660.927	-1			
5662.157	1		.162	0
5662.930	3	Ti Fey II	.942	1
5663.999	1	Ni Cr	.012	1N
5664.600	-1		.586	-2
5667.162	2	Sc II	.157	0
5668.394	-1	Vi I	.382	-2
5668.905	1	Ce II	.919	-3
5669.065	1	Sc II	.043	1
5669.970	1	Ni I	.951	0
5670.868	1	V I	.859	0
5671.823	2	Sc I	.835	0
5673.057	-2	Ti I	.060	-3
5673.421	-1	Ti I	.422	-2N
5674.068	-2			
5674.175	-2	Cr I	.174	-3
5674.508	-2			
5675.444	1	Ti I	.437	2N
5675.866	-1			
5676.359	-2	Nd	.355	-3
5676.572	-2			
5677.199	-1			
5677.501	-2		.466	-3
5678.142	-2		.063	-3
5678.296	-2			
5679.329	-2		.287	-3N
5679.723	-2			

Observed	Intensity	Element	Rowland	Rowland Intensity
5679.908	+1	Ti I	.934	-2
5680.305	-2	Fe I	.255	1
5680.819	-2			
5680.917	-2	Zr I	.91	-2
5681.256	-2	Cr I	.247	-2
5682.200	-1	Ni I	.211	2
5683.773	-1			
5683.986	-1		.904	-3
5684.196	3	Sc II	.201	1
5685.852	-1	Fe I	.887	-2
5686.215	-1	Fe I	.216	0
5686.850	1	Sc I	.850	-2
5688.531	2	Nd II	.546	-3
5689.464	1	Ti I	.480	0
5690.032	-1	Fe I	.074	-3
5690.131	-1		.074	-3
5694.747	1	Cr I	.747	0
5694.990	1	Ni I	.994	2
5695.861	0			
5696.266	-2	Sm ?		
5696.706	-2	Sm ?	.657	-3N
5698.113	-1			
5698.308	1	Cr I	.343	1
5698.534	2	V I	.533	1
5700.151	1	Sc I	.190	-1
5700.507	-1	Cr I	.526	-2

Observed	Intensity	Element	Rowland	Rowland Intensity
5700.617	-1			
5702.241	0	Nd II		
5702.668	1	Ti I	.661	-2
5703.329	-1	La II	.379	-3
5703.586	2	V I	.590	1
5704.380	0		.396	-3
5705.319	-1	Fe I	.312	-3
5705.971	0		.011	0
5706.190	1	Nd II	.116	0
5706.704	-1		.728	-1N
5706.965	0	V I	.991	0
5708.262	2	Nd II		1
5709.695	0			
5709.841	0		.792	-2
5710.147	-1			
5711.211	-1			
5711.439	0	Ce II	.401	-2d
5711.670	-1			
5711.758	1	Sc I		
5712.631	-1	Cr I	.621	-2
5712.923	-1			
5713.126	-2			
5713.424	-2		.456	-2
5713.890	1	Ti I	.904	-2
5714.842	-2	Fe I	.903	-3
5715.051	0	Ni-Fe-Ti	.097	5
5715.261	0			

Observed	Intensity	Element	Rowland	Rowland Intensity
5716.435	1	Ti I	.458	-1
5718.138	1	Nd II	.125	-2N
5718.280	0		.297	-2N
5718.598	0			
5720.097	-1		.062	-3
5720.405	1	Ti I	.355	-2
5720.614	0	Y I ?		
5721.080	-2		.054	-3
5721.659	-1		.717	-1
5721.828	-1		.834	-2
5722.083	0			
5723.285	-2			
5723.524	0		.543	-3
5723.795	-1	Mn ?	.777	-2
5724.062	-1	Sc I	.101	-2
5724.289	-1			
5725.616	-1	VI	.668	-2
5725.963	-1	Fe II	.956	-2d
5726.805	1			
5727.038	1	V I	.060	2N
5727.281	0	La II	.293	-3N
5727.655	0	VI	.661	-1
5728.907	0	Y II	.884	-1d
5729.214	-1	Cr I	.205	-2
5729.950	-1		.904	-3
5731.201	0	VI	.226	-1

Observed	Intensity	Element	Rowland	Rowland Intensity
5731.332	0	VI	.324	-1
5732.179	-1		.124	-3
5732.279	-1	Fe I	.311	0
5732.393	-1		.311	0
5732.535	-1			
5732.718	1	Fe II	.737	-2
5733.249	0			
5733.391	0		.339	-3
5733.854	0	Ce II	.895	-2
5734.042	-1	V I	.051	-2
5734.530	0		.575	0
5736.626	-1	Cr I	.647	-3
5736.832	-2			
5737.060	1	V I	.077	0
5738.115	-2			
5738.373	-1	Mn I	.242	0
5739.475	0	Ti I	.486	0
5739.975	0	Ti I	.988	0
5740.864	1	Nd II	.878	-2
5741.230	0	Ti I	.222	-2
5742.096	1	Nd	.083	-2
5742.538	-1		.575	-2N
5743.192	-1	Nd	.200	-1d
5743.451	1	V I	.435	-1
5743.642	-1			
5743.888	-1	Y I	.942	-1
5744.133	-1	Nd	.206	-3

Observed	Intensity	Element	Rowland	Rowland Intensity
5744.746	1	Nd		
5745.233	-2			
5745.420	0			
5746.983	-1			
5747.190	0			
5747.434	0			
5747.696	0	Mo	.672	1
5747.863	0	Fe I	.865	-2
5748.148	1	Fe I	.170	-2d
5748.497	0		.527	-3
5752.862	0	Ti I		
5753.060	0		.135	5
5753.312	0	Fe I		
5753.524	0	Nd		
5754.105	0	Co I	.098	-2
5754.316	0			
5754.536	0			
5754.966	-1	Fe I	.923	-2N
5755.585	-1			
5755.909	0			
5756.191	0		.200	-3
5756.674	-1			
5758.783	-1		.768	-2
5759.057	-1			
5759.302	-1	Fe I	.278	0
5759.424	-1			
5760.510	-1	Fe I	.538	-2

Observed	Intensity	Element	Rowland	Rowland Intensity
5760.647	-1		.704	-3
5760.831	0	Ni I	.843	2
5761.723	1	Sm		
5762.300	2	Ti I	.268	2d
5762.567	0		.629	-1N
5762.757	0	Fe I ?	.847	0
5762.918 dr	0	Fe	.005	6
5763.179	0			
5764.283	-2			
5766.331	2	Ti I	.337	0
5768.879	1	Ce II	.909	-2N
5769.077	2	La II	.084	-2
5769.269	-1		.336	0
5769.842	-1	Nd		
5769.977	-1	La I		
5770.155	-1	Fe I		
5770.412	-1	Ce		
5770.511	0		.503	-2d
5771.625	-1	Cr	.609	-1
5772.415	1	V I	.419	-2
5772.868	0	Ce		
5773.071	0	Ce ?		
5774.040	2	Ti I	.039	0
5774.264	-1			
5774.678	-1			
5775.712	-1			
5780.919	0	Cr I	.920	-1

Observed	Intensity	Element	Rowland	Rowland Intensity
5781.187	0	Cr I	.190	0
5781.731	2	Cr I	.757	0
5782.029	0			
5782.608	-1	V I	.605	-2N
5783.059	1	Cr I	.077	2
5783.667	0	Nd	.678	3
5783.863	1	Cr	.870	3
5784.353	0	V I	.395	-2N
5784.797	0		.826	-2
5784.980	0	Cr	.980	2
5785.140	0			
5784.441	-1			
5785.730	0	Cr	.739	1
5785.987	2	Cr - Ti	.983	0N
5786.171	0	VI	.163	-2
5786.762	-2		.754	-3N
5787.048	-2	Cr I	.024	-1
5787.913	2	Cr I	.930	4
5788.067	0			
5788.270	0	Nd ?		
5788.374	0	Cr I	.400	-1
5788.493	0	VI ?		
5788.684	1		.654	-3
5788.928	0			
5789.018	0			
5789.338	0		.354	-3

Observed	Intensity	Element	Rowland	Rowland Intensity
5789.430	0			
5789.603	0	Fe	.639	-3
5789.782	0		.767	-3
5789.972	0		.925	-3
5790.164	0		.196	-1
5790.254	0			
5790.945	1	Cr	.963	4
5791.190	0		.194	-2
5791.390	-1		.409	-3
5791.784	-1	Cr I	.763	-2
5791.881	-1	Mo I		
5792.882	-1		.874	-3
5793.364	-1		.399	-2
5794.883	-2		.875	-3
5795.016	-1		.001	-2
5795.154	-1			
5796.771	-1	Cr I	.774	-1
5797.412	0	Ti I		
5797.584	2	La II	.604	-2
5797.739	-1	Zr I	. 75	0
5798.071	0	Fe I	.186	4
5798.359	0	Fe I	.186	4
5799.328	-2			
5799.805	0	Ce		
5800.214	-2		.232	-2d
5800.559	-1			
5801.159	-1	Cr I		

Observed	Intensity	Element	Rowland	Rowland Intensity
5803.233	-1			
5803.440	0			
5803.985	1	Mo	.042	1
5804.255	3	Ti I	.270	0
5804.557	0			
5805.039	-1			
5805.212	1	Ni I	.228	4
5805.768	2	La II	.774	0
5806.199	-1	Mo		
5806.395	-1	Nd		
5806.583	0	La II	.535	-3
5807.110	0	V I	.097	-2
5807.625	0		.597	-3N
5808.310	0	La II	.314	3
5808.556	-2		.569	-3N
5808.807	-1			
5809.434	-1		.458	-2N
5809.643	-1		.618	-2N
5811.581	2	Nd II	.611	-2d
5812.317	-1			
5812.834	0	Ti I	.848	-2
5812.968	0	Ce		
5813.741	0		.672	-2
5815.145	-1	Fe I		
5815.383	0	Fe I		
5815.860	0		.874	-2
5816.143	-1			

Observed	Intensity	Element	Rowland	Rowland Intensity
5816.278	0		.269	-1
5816.521	-1			
5816.727	-1			
5817.154	-1	.087	.087	0
5817.489	0	VI ?	.496	-2
5818.020	-1			
5818.562	-1			
5818.776	-1			
5819.039	-1			
5819.922	-1		.933	-1
5820.122	-2			
5821.005	-1			
5822.470	1		.468	-1N
5873.159	0	V	.176	-2
5823.353	0	Nd	.363	-3
5823.679	0	Ti I	.698	-1
5823.946	0	Cr Cl ?		
5824.415	0	Fe II	.416	-1
5824.802	-1		.764	-1
5825.878	1	Nd		
5826.313	0	Co I	.334	-2
5826.628	0	Fe I	.649	-2N
5826.929	-1	Mo		
5828.052	-1			
5828.516	-1	La II		
5830.047	1	Co I	.987	-3
5830.689	1	V I	.684	-2

Observed	Intensity	Element	Rowland	Rowland Intensity
5831.605	0	Ni I	.610	1
5831.783	0	Sm II	.756	
5832.485	0	Ti I	.480	-2
5833.688	-2		.675	-3N
5834.548	0	Nd	.545	-2
5834.781	-1	Fe		
5838.030	1		.014	-2
5838.522	0			
5839.582	0	Sm ?	.612	-1
5840.946	-1			
5841.211	0		.194	-2
5842.382	2	Nd II	.389	-2
5843.725	-1	Ce		
5844.075	-1			
5844.301	-1			
5845.401	0			
5845.655	0			
5846.269	2	V I	.276	-1
5847.131	1	Pr ?		
5848.888	0			
5851.397	-2			
5852.697	-2			
5853.611 dr 5853.780	0 0	Ba II	.691	5
5854.027	-1			
5854.316	-1	Sc II	.324	-2

Observed	Intensity	Element	Rowland	Rowland Intensity
5856.944	-1	Gd II ?		
5857.338 dr	-1	Ca	.462	8
5857.590	0			
5857.760	0	Ni I	.762	3
5858.565	-1	Ce II	.539	-2N
5858.959	-1	Nd ?	.004	-2N
5859.749 rf	0	Fe	.600	5
5860.256	-1			
5860.793	-1	Sm ?		
5863.077	-1			
5863.378	-1			
5863.718	2	La II	.722	-3
5864.268	-1	Fe	.252	0
5864.464	-1			
5865.048	-1	Nd		
5865.321	-2			
5867.137	-2		.091	-1N
5868.888	-1	Nd		
5869.495	-1	Zr I		
5871.072	-1	Sm ?		
5871.661	-1			
5871.948	-1			
5873.877	-1	Ce		
5874.019	-1	La II		
5874.571	-1			
5874.761	-1		.783	-3N
5875.543	1	He I	.618	

Observed	Intensity	Element	Rowland	Rowland Intensity
5875.715	4			
5877.686	0		.691	-3
5879.315	0		.294	-3
5880.645	-1	La II	.620	-3
5881.604	-1		.548	-3
5889.777 dr.	3	Na I	.977	30
5890.176	1			
5892.169	-1			
5893.843	-1		.838	-3
5894.512	0			
5894.727	-1			
5895.766 dr	1	Na I	.944	20
5896.117	2			
5896.741	-1			
5898.521	-1		.533	-3
5898.714	-1			
5899.523	-1		.540	-1
5901.938	-1	La II		
5902.383	1			
5902.758	0	Eu ?		
5903.182	0		.122	-3
5904.523	-1	Gd ?		
5904.991	-1		.936	-3
5905.482	0		.440	-3
5905.700	0	Fe I	.684	4
5906.644	0	Nd	.652	-3

Observed	Intensity	Element	Rowland	Rowland Intensity
5907.585	0			
5908.494	-1			
5908.737	-1		.733	-3
5911.120	-1		.153	-3
5913.949	0		.906	-3
5914.397	0			
5914.607	-1	.	.638	-3
5916.512	0			
5916.894	-2	Co I		
5917.117	-2			
5917.875	0		.810	-3
5918.138	1			
5918.559	-1	Ti I	.562	
5918.862	-1	Fe I		
5919.207	-1		.293	-3
5920.089	-2			
5920.300	-1		.334	-3
5923.422	-1	Fe ?	.489	-3
5926.199	0	Cr II ?	.205	-3
5926.977	0			
5928.615	0			
5928.729	0	Ce		
5930.362	0			
5933.172	-1		.212	-3
5933.398	-1			
5933.575	0	Ce		
5934.284	-1		.277	-3

Observed	Intensity	Element	Rowland	Rowland Intensity
5934.903	-1		.952	-3
5936.009	0		.065	-3
5936.527	-1			
5937.734	0	Ce		
5937.879	-1	Ti I	.822	-2
5938.224	0			
5938.530	0			
5938.731	-1	Fe	.752	-3
5939.732	-2	Nd	.754	-3
5940.103	-1			
5940.803	0	La I?		
5941.394	1	Fe II ?	.417	-3
5941.946	-1			
5942.153	-1		.186	-3
5942.804	0		.737	-3
5942.985	0	Sm ?	.907	-3
5943.430	0		.392	-1
5943.703	0			
5946.560	0			
5947.219	1	Pr ?	.287	-3
5949.555	1			
5950.778	0			
5951.133	1		.096	-3
5951.441	1			
5951.635	1	Gd II ?		
5952.231	-1	Fe I	.192	-3
5952.601	0		.526	-2

Observed	Intensity	Element	Rowland	Rowland Intensity
5952.920	-1		.993	-3N
5953.050	0	Nd		
5953.165	0	Ti I	.174	1
5954.534	0			
5957.108	0			
5957.336	0			
5960.153	-1	Ce ?		
5960.761	-1			
5961.065	-1			
5961.664	0			
5962.054	-1			
5963.506	0		.575	-3
5965.252	0			
5965.861	0	Ti I	.840	2
5968.540	-1			
5969.485	-1	Sm ?	.580	-2
5969.851	0			
5970.422	0		.498	-3
5970.806	-1	Sm ?		
5971.121	-1		.150	-3
5972.241	0			
5972.468	-1	Nd ?		
5974.613	-1	Fe I	.596	-3N
5975.848	1	Ce II	.830	-3
5978.078	0		.076	-3
5978.296	0			
5978.573	1	Ti I	.554	1

Observed	Intensity	Element	Rowland	Rowland Intensity
5979.345	-1	Cr II	.311	-3
5979.548	-1			
5982.474	-1			
5984.478	-1			
5984.687	0	V I		
5988.906	-1		.965	-3
5989.060	0			
5989.715	-1			
5989.916	-2			
5991.403	5	Fe II	.383	2
5993.853	-1	Gd		
5994.048	-1	Nd		
5995.153	-1			
5995.450	-1			
5995.662	-1	Ti I	.701	-3
5995.873	-1			
5996.626	-1			
5996.783	-1	Ni I	.745	1
5999.061	-1	Gd ?		
5999.412	-1		.432	-3N
6000.692	-1	Co I	.686	-1
6000.986	-1			
6005.718	1		.789	-3
6005.972	-1			
6006.367	1			
6007.675	-1		.722	-2

Observed	Intensity	Element	Rowland	Rowland Intensity
6008.474	0			
dr		Fe I	.572	6
6008.706	0			
6012.090	0			
6013.360	0			
dr.		MN	.503	6
6013.671	1			
6016.287	0	Nd		
6016.514	1			
dr		MN	.653	6
6017.816	1			
6018.483	-1	Ti I	. 41	-3
6018.859	-1		.829	-3
6019.294	0			
6019.538	-1		.585	-3N
6020.676	-1		.663	-3
6021.014	-1			
6021.660	0			
dr		MN	.808	6
6021.988	0			
6022.586	-1			
6023.415	-1	YI	. 42	0
6023.762	-1			
6026.965	0			
dr		Fe I	.064	4
6027.201	0			
6027.954	-1			
6029.191	-1			
6029.944	0		.901	0
6030.278	-1		.341	-3
6030.496	-1			
6030.693	-1	Mo I	. 69	0

Observed	Intensity	Element	Rowland	Rowland Intensity
6031.444	-1			
6033.569	2	Ce II	.602	-3N
6034.213	2	Ce II	.232	-3
6039.727	1	V I	.745	0
6041.652	-1			
6043.377	3	Ce II	.432	-2
6044.787	-1			
6045.021	-1			
6047.484	-1			
6048.734	1			
6049.096	1	Co I	.129	-2N
6049.495	0	Gd II		
6051.838	0	Nd	.853	-3N
6052.586	0	Ce II	.620	-2
6053.301	0		.268	-3N
6053.851	0	Sm ?	.917	-3
6055.053	-1		.102	-2
6055.205	-1			
6055.759	-1		.772	-3N
6056.373	-1		.357	-2
6056.709	0		.779	-3N
6057.375	0	Eu ?		
6057.685	0	Sm ?		
6057.837	0		.872	-3
6058.490	-1			
6058.933	-1			
6059.394	-1			

Observed	Intensity	Element	Rowland	Rowland Intensity
6060.961	-1			
6062.756	0	Cr I	.702	-2
6063.011	0		.872	0
6063.556	-2			
6063.832	-2	Mo ?		
6064.018	-2		.051	-2N
6064.345	-1			
6064.485	0			
6064.755	0			
6065.388	0			
6065.614	0			
6067.282	0	V I	.285	-3
6067.506	0			
6067.731	0	Sm ?		
6069.654	0	Nd		
6071.510	0			
6073.981	1	Nd	.023	-3
6074.790	-1			
6075.804	-1			
6075.908	-1			
6076.913	0		.913	-1
6077.241	-1	Nd	.273	-3N
6077.522	-1	Ce II	.495	-3N
6077.959	-2			
6079.293	-1			
6080.239	-1		.243	-3
6080.618	-1	Nd	.587	-3N

Observed	Intensity	Element	Rowland	Rowland Intensity
6081.448	2	V I	.458	0
6082.415	0	Co I	.433	2d
6084.107	4	Fe II	.118	0
6085.072	-1			
6085.477	-1	La II	.449	-3
6086.287	1	Ni I	.294	1
6086.680	1	Co I	.678	-3N
6086.972	0	Nd		
6087.543	0	Nd		
6087.832	0		.840	1N
6088.966	-1	Ce		
6089.169	-1			
6089.416	0	V I		
6089.702	-1	Cr II ?	.580	1
6090.212	2	V I	.222	2
6091.177	1	Ti I	.182	0
6091.544	-1		.507	-3
6091.920	0		.927	1
6092.164	-1			
6092.467	-2		.530	-3
6092.664	-1			
6094.237	0			
dr		Fe	.383	1
6094.527	0			
6097.166	-1		.106	-3
6097.388	0			
6098.114	-1			
6098.352	0			

Observed	Intensity	Element	Rowland	Rowland Intensity
6098.664	1	Ti I	.664	-1
6100.104	1			
6100.389	1	La II		
6101.229	0			
6102.343	0			
6102.585	1			
dr		Ca I	.733	9
6102.872	0			
6103.929	-2			
6104.429	-2			
6104.856	-1			
6105.243	0			
6106.470	1	Zr II	.446	-3
6107.067	-1	Fe I	.104	-3
6107.355	-1	Fe I	.355	-3
6107.890	0	Co I	.903	-3
6108.752	-1	Ce		
6111.651	2	V I	.668	0d
6113.324	3	Fe II	.334	0
6113.795	-1			
6114.272	-1			
6114.557	-1			
6114.799	1	Zr II	.806	-3
6116.051	1	Fe II	.064	-3
6116.185	0	Ni I	.193	1
6116.362	0			
6116.760	-2		.696	-3d

Observed	Intensity	Element	Rowland	Rowland Intensity
6117.182	0		.211	-2
6119.533	2	V I	.537	1
6119.776	0	N I	.767	0
6120.485	-2		.548	-3
6121.731	0		.783	-3
6121.932	0			
6122.642	0	Co I	.627	-2
6126.096	1	La II		
6126.357	-1			
6127.460	-1	Zr I	.481	-3N
6127.630	-1		.649	-3
6127.807	0	Fe	.918	3
6128.021	0			
6128.551	-1			
6128.790	-1			
6129.101	-1			
6129.254	-1	Mn II	.228	-2
6129.552	0	La II	.538	-2N
6129.708	1	Fe II	.738	-2
6129.929	0		.943	-3
6130.135	1	Ni I	.147	1
6132.678	-1			
6132.814	-1		.818	-3N
6133.553	-1		.583	-3N
6135.366	2	V I	.378	1N
6136.517	0			
6137.150	-1			

Observed	Intensity	Element	Rowland	Rowland Intensity
6137.376	0	Nd		
6137.583	-1			
dr		Fe I	.709	7
6137.917	0			
6138.541	0		.524	-1N
6141.028	-1	Fe II	.064	-2
6141.627	4			
dr		Ba II-Fe I	.733	7
6141.810	4			
6143.215	-1	Zr I		
6143.376	1			
6145.438	-2	Fe I	.415	2N
6145.945	-2			
6146.216	-2	Ti I	.244	-2
6147.732	3	Fe II	.749	2
6149.241	4	Fe II	.255	2
6150.121	1	V I	.158	0Nd
6150.270	-1	Nd		
6150.468	-1			
6151.454	0			
6151.759	0	Ce		
6153.183	0			
6155.882	0			
dr		Ti I - Ca I	.037	-1
6156.165	0			
6156.962	-1			
6157.309	0			
6157.596	1			
dr		Fe I	.739	5
6157.859	1			
6158.171	0		.177	-2N

Observed	Intensity	Element	Rowland	Rowland Intensity
6158.920	0	Ce		
6159.176	0			
6159.858	-1	Ce		
6160.041	-1			
6160.368	-1			
6160.886 rf	1	Na I	.759	3
6161.170 dr	1	Ca I	.302	4
6161.406	1			
6161.824	0			
6162.533	-1			
6163.339	-1			
6163.424	0	Ni I	.426	2
6164.383	0			
6164.784	-1			
6165.259 dr 6165.504	0	Fe I	.369	3
6165.965	0	Pr II ?	.901	-3
6166.271	0		.206	-3
6170.349	0	V I		
6170.499	0	Fe I	.522	6
5161.249	-2		.238	-3
6172.546	-2			
6172.730	-2	La II	.740	-3N
6173.027	-1		.071	-3N
6174.181	-2	La II		
6175.359	1	Ni I	.376	3

Observed	Intensity	Element	Rowland	Rowland Intensity
6181.009	-1			
6182.321	0			
6183.670	-2			
6183.898	1	Ni I	.875	-2
6185.902	-1			
6186.202	-1	Ti I	.219	-1N
6187.251	-1			
6188.695	-2			
6189.644	-2			
6191.474	1			
dr		Fe I	.577	9
6191.678	-1			
6193.412	-1			
6193.731	-2			
6194.403	-1	Sm ?	.429	0N
6195.451	-1		.459	0N
6198.619	-2	Nd	.661	-3
6199.199	1	V I	.195	0
6200.874	-2			
6201.765	-2	Nd		
6203.348	0		.351	-3
6205.230	-2			
6205.619	-2			
6206.156	-2			
6207.985	-2			
6208.554	-2		.580	-1

Observed	Intensity	Element	Rowland	Rowland Intensity
6201.667	1	Se II	.693	-1N
6211.186	-1	Co I		
6212.219	0	Ti II	.277	-3
6213.126	-1			
6213.348	0			
6213.864	0	V I	.878	-2
6214.400	-1			
6214.662	-1	Zr ?	.683	-2N
6214.881	-1			
6215.038	-1			
6215.246	1	Ti I	.26	3
6215.592	-2			
6216.083	-1			
6216.367	0	V I	.366	1
6217.974	-2	Fe II		
6218.290	-1			
6218.911	-2			
6219.201	0			
rf		Fe I	.294	6
6219.543	-1			
6219.937	-1	Ti I	.949	-3
6220.469	1	Ti I	.499	-2
6221.296	1	Ti - Fe	.351	1d
6221.813	0			
6221.981	0			
6223.370	-2	Co I	.451	-3N
6224.512	0	V I	.514	-2
6226.275	-2		.326	-3N

Observed	Intensity	Element	Rowland	Rowland Intensity
6229.357	1	Fe II	.240	1
6230.258	-1			
6230.435	-1			
6230.635	0			
dr		Fe I	.742	8
6230.827	0			
6231.036	-2		.009	-3
6231.318	-1			
6232.437	1	Co I		
6233.181	-1	V I	.206	-2
6233.525	-1	Fe II	.518	-3d
6236.266	-2			
6238.386	4	Fe II	.396	2
6239.359	1	Fe II	.382	-1
6239.771	-1	Sc I	.777	-3
6239.944	1	Fe II	.962	-1
6242.822	0	V I	.852	-2
6243.106	1	V I	.120	1
6243.340	-1		.337	-3N
6244.300	-1	Pr II ?		
6245.485	1			
6245.660	1	Sc II		
6247.299	-1	Co I		
6247.559	3	Fe II	.569	2
6248.279	-1	Nd		
6248.911	0	Fe II	.919	-2
6250.443	0	Nd		
6251.821	1	V I	.845	-1

Observed	Intensity	Element	Rowland	Rowland Intensity
6252.475 dr	1	Fe I	.572	7
6252.654	0			
6253.700 dr	-1	Fe I	.847	-1
6253.972	0			
6254.747	-2	Fe	.797	-3N
6255.097	-2			
6255.592	-2	Sc I ?	.603	-3N
6256.921	-1	V I	.888	-3N
6257.574	1	Co I	.600	-3N
6258.960	1	Sc I	.942	-3
6259.382	-1			
6259.754	0	Gd ?	.778	-3
6261.464	-1			
6262.187	1	Sc I ?		
6262.419	1			
6262.926	0		.962	-3N
6264.364	-1			
6264.523	-1			
6266.332	0	V I	.348	-2
6266.718	-1			
6266.980	-1			
6267.243	-1		.222	-3N
6268.521	-1	Ti I		
6268.841	0	V I	.878	-2N
6269.966	1		.998	-2
6271.489	1	Co I	.501	-3

Observed	Intensity	Element	Rowland	Rowland Intensity
6272.030	1	Ce		
6272.920	-1			
6273.122	-1	Sc I ?	.104	-3N
6273.562	-1			
6273.774	0	La II		
6274.662	1	V I	.668	-1
6276.329	0	Sc I		
6284.792	0	Sc I	.790	-3
6284.968	-1			
6285.177	1	V I	.181	-1N
6286.149	0		.156	0
6288.043	-1	Nd		
6289.869	-1		.903	-3N
6291.853	-1	Co I		
6292.847	1	V I	.827	-2
6293.782	0			
6295.438	-1		.387	-3
6295.675	-1			
6296.087	1	La II	.156	-3
6296.499	1	V I	.511	-3
6299.621	1	Sm ?	.601	0
6307.520	0		.558	-3N
6307.755	0		.885	-2N
6312.998	0	Zr I		
6313.533	0	Zr II		
6320.401	2	La II	.453	-2

Observed	Intensity	Element	Rowland	Rowland Intensity
6326.847	0	V I	.830	-3
6328.195	0			
6328.584	-1			
6341.445	-1b			
6346.513	0	Zr II		
6347.109	6	Si II	.104	2N
6347.852	1	Co I	.875	-2
6349.471	0	V I	.49	0
6351.436	0	Co I		
6357.285	0	V I	.30	0
6359.262	-1		.234	-3
6361.415	0	Ti I		
6362.102	0	Nd		
6362.357	0	Zn I	.357	1
6363.805	0	(0 I)		
6364.825	-1			
6365.551	-1			
6367.290	-1			
6369.460	5	Fe II	.479	0
6371.114	1	Ce		
6371.375	5	Si II		
6374.145	-1	La II		
6378.031	-1		.180	-3
6381.658	0		.639	-3
6382.082	0	Nd		
6383.731	0	Fe II	.726	0N

Observed	Intensity	Element	Rowland	Rowland Intensity
6384.058	-1			
6385.197	0	Nd II	.097	-3N
6385.461	-1	Fe II	.474	-2N
6390.489	2	La II	.509	-2
6393.033	0	Ce		
6393.391	0	V I		
6395.122	0	Ca I ?	.172	-1d ?
6396.548	0	Co I		
6399.050	0	La II		
6407.251	1	Fe II		
6412.819	0			
6413.366	0	Sc I	.33	
6413.752	0			
6416.924	4	Fe I	.935	1
6417.420	-2			
6417.697	-2		.696	-1N
6421.265	0			
6425.284	-1	Ce		
6425.791	-1	Nd		
6426.587	-1	La I		
6428.662	0	Nd	.639	-3
6429.635	0	Pr ?		
6430.217	-1			
6430.483	-1	V I	.461	-3
6431.851	0			
6432.159	-1			
6432.696	3	Fe II	.690	1

Observed	Intensity	Element	Rowland	Rowland Intensity
6433.195	-1	VI		
6433.599	1			
6433.797	1			
6442.980	0	Fe II	.976	-2
6450.497	0			
6455.018	1	Co I	.024	0N
6456.391	6	Fe II	.396	3
6466.877	-1			
6477.888	0	Co I	.901	-2N
6491.584	1	Ti II	.590	1
6492.37	-1			
6494.883	0	Fe I		
6496.808 dr	4	Ba II	.916	4
6497.017	4			
6498.194	-1	La II	.194	-3N
6502.734	-1			
6503.268	-1			
6516.091	6	Fe II	.094	2
6526.980	0b	La II		
6548.326	-1			
6554.852	0		.857	-3N
6559.587	2	Ti II	.588	0
6563.	50	H	.816	40
6565.533	0	Ti I ?	.53	
7771.950	10	OI	.954	2
7774.177	8	OI	.177	2
7775.397	6		.394	--